JOURNAL OF
SYMPLECTIC GEOMETRY
Volume 22, Number 5, 1109–1178, 2024

Rational cuspidal curves and symplectic fillings

Marco Golla and Laura Starkston

A symplectic rational cuspidal curve with positive self-intersection number admits a concave neighborhood, and thus a corresponding contact manifold on the boundary. In this article, we study symplectic fillings of such contact manifolds, providing a complementary perspective to our earlier article on symplectic isotopy classes of rational cuspidal curves. We explore aspects of these symplectic fillings through Stein handlebodies and rational blow-downs. We give examples of such contact manifolds which are identifiable as links of normal surface singularities, other examples which admit no symplectic fillings, and further examples where the fillings can be fully classified.

1. Introduction

In [GS22], we studied *symplectic rational cuspidal curves* in closed symplectic 4-manifolds up to equisingular symplectic isotopy (see also [GK22] for an extensions of those results for curves in $\mathbb{CP}^2$). Rational means the geometric genus is zero, and cuspidal means that the singularities are locally irreducible and modeled on the singularities of complex curves. The link of a cuspidal singularity is an algebraic knot, and we primarily focus on cases where the link is a torus knot $T(p,q)$.

In this article we explore the symplectic and contact geometry associated with rational cuspidal curves from a complementary perspective. Namely we look at the symplectic fillings found as the complement of a neighborhood of such a curve in some closed symplectic 4-manifold. We showed in [GS22, Theorem 2.13] that if C is a singular symplectic curve of positive self-intersection, it has small concave neighborhoods, whose contact boundary we will denote by (Y_C, ξ_C). Note that this contact structure depends only on the topological types of the singularities, geometric genus, and self-intersection number of C. In this article, we will study properties of these contact manifolds and their symplectic fillings for many examples of (neighborhood germs of) rational curves C, specified by their singularity types and self-intersection number. We describe some situations where such contact manifolds admit no fillings, and others where the fillings can be completely classified and described explicitly.

Note that any symplectic filling of (Y_C, ξ_C) can be viewed as the complement of a neighborhood of a symplectic embedding of C in a closed symplectic 4-manifold (obtained by gluing the concave neighborhood of C to the filling). Although our prior work gives classification results for embeddings for many such rational cuspidal curves and thus yields abstract classifications of the symplectic fillings of (Y_C, ξ_C), more work is required to determine concrete diagrammatic presentations for these symplectic fillings and to explore the relations between different fillings. We take on these problems in this article.

We start with a study of the fillings of (Y_C, ξ_C) where C is a rational cuspidal curves with a unique singularity modeled on $\{x^a = y^b\}$ (whose link is the torus knot $T(a,b)$) which embeds into $\mathbb{CP}^2$ in the homology class $d[\mathbb{CP}^1] \in H_2(\mathbb{CP}^2)$. Note in this case, the corresponding self-intersection number is d^2. According to [Liu14, Theorem 2.3] (see also [BCG16, Remark 6.18]), all such C belong to the list of [FLMN07, Theorem 1.1]; namely,

$(p, q; d)$ is one of:

$$\begin{array}{lll} \mathcal{A}_p : (p, p+1; p+1), & (F_{j-2}, F_{j+2}; F_j), & \mathcal{E}_3 : (3, 22; 8), \\ \mathcal{B}_p : (p, 4p-1; 2p), & (F_j^2, F_{j+2}^2; F_j F_{j+2}), & \mathcal{E}_6 : (6, 43; 16). \end{array}$$

Here F_i denotes the i^{th} Fibonacci number. The two Fibonacci families correspond to curves C where (Y_C, ξ_C) is either a universally tight lens space or a connected sum of universally tight lens spaces. In these cases, the fillings have been previously classified, some of them have been presented through Stein handle diagrams and Lefschetz fibrations, and their rational blow-down relations have been established [Hon00, Lis08, LM14, BO16]. We denote the remaining two infinite families with $\mathcal{A}_p$ and $\mathcal{B}_p$, corresponding to $(a, b) = (p, p+1)$ (and degree $p+1$) and $(a, b) = (p, 4p-1)$ (and degree $2p$), respectively. The two exceptional cases, corresponding to $(a, b) = (3, 22), (6, 43)$ (of degrees 8 and 16) are denoted with $\mathcal{E}_3$ and $\mathcal{E}_6$. We find presentions for each of the corresponding contact manifolds (Y_C, ξ_C) as the boundary of a Stein handlebody diagram.

Theorem 1.1. *Let C be a rational cuspidal curve in $\mathbb{CP}^2$ with one cusp of torus knot type.*

- *If C is of type $\mathcal{A}_p$, then the unique minimal symplectic filling of ξ_C has the Stein handlebody diagrams shown in Figure 1, so (Y_C, ξ_C) is specified by the corresponding contact surgery diagram.*
- *If C is of type $\mathcal{B}_p$, then the two minimal symplectic fillings are given by Stein handlebodies in Figures 4 and 5, so (Y_C, ξ_C) is specified by the corresponding contact surgery diagrams.*
- *If C is of type $\mathcal{E}_3$ or $\mathcal{E}_6$, then ξ_C is the canonical contact structure on Y_C given as the link of a normal complex surface singularity whose minimal resolution is symplectic deformation equivalent to the Stein manifolds whose handle diagrams are shown in Figures 9 and 11, thus yielding contact surgery diagrams for the corresponding contact manifolds.*

In the $\mathcal{A}_p$ and $\mathcal{B}_p$ cases, to prove the Stein handlebodies we present have contact boundaries agreeing with (Y_C, ξ_C), we use Kirby calculus to identify the smooth boundary of the handlebody with Y_C, and an argument using Gompf's Γ-invariant [Gom98] of contact structures and results of Matkovič [Mat18] to identify the contact boundary of the Stein handlebody with ξ_C. The key technical tool is a general computation of Gompf's

Γ-invariant for the contact manifolds (Y_C, ξ_C) when C is an arbitrary rational cuspidal curve (Theorem 2.1).

In the $\mathcal{E}_3$ and $\mathcal{E}_6$ cases, to identify the contact structure as the canonical structure from a complex surface singularity we use classification results of Ghiggini [Ghi08, Theorem 1.3] (see also [Tos20] for a more general statement) and Heegaard Floer correction terms.

Next we consider relations between different symplectic fillings of the same (Y_C, ξ_C). We focus on when such fillings are related by *rational blow-down*, a surgery operation introduced by Fintushel and Stern [FS97] and generalized by Park [Par97] and Stipsicz, Szabó, and Wahl [SSW08]. Because its effect on Seiberg–Witten invariants has been established, rational blow-down has proven a very useful tool to produce small exotic 4-manifolds (see [Par05, SS05, PSS05, FS06] as a small sample of the many examples in the literature). When we have multiple symplectic fillings of a given contact manifold, we can ask whether they are related via a known rational blow-down operation, or whether the substitution of fillings yields a new symplectic cut-and-paste operation. In the case of lens spaces with the canonical contact structure Bhupal and Ozbagci proved that all symplectic fillings are obtained from a plumbing by a sequence of symplectic rational blow-downs [BO16]. We prove the analogous result for the cases of (Y_C, ξ_C) considered above: every minimal symplectic filling can be obtained from the largest filling by a sequence of symplectic rational blow-downs (where we include generalized rational blow-downs of [Par97] and [SSW08]).

Theorem 1.2. *Let C be a rational unicuspidal curve in $\mathbb{CP}^2$ whose singularity link is a torus knot.*

- *If C is of type $\mathcal{B}_p$, the two fillings of (Y_C, ξ_C) differ by rationally blowing down a symplectic -4-sphere (or rationally blowing up a Lagrangian $\mathbb{RP}^2$).*
- *If C is of type $\mathcal{E}_3$ or $\mathcal{E}_6$, one filling is given by a symplectic plumbing of spheres and every other filling is obtained from this plumbing by a sequence of symplectic rational blow-downs.*

In the $\mathcal{E}_3$ and $\mathcal{E}_6$ cases, we specify precisely which pairs of fillings are related by a rational blow-down. In each case, there are pairs of fillings which cannot be related by rational blow-downs—instead one must first rationally blow-up one of the fillings to get to a larger filling and then rationally blow-down to get to the second filling.

Generalizing from the case of unicuspidal C which embed in $\mathbb{CP}^2$, we can consider more general rational cuspidal curves and the corresponding contact manifolds (Y_C, ξ_C). We specify the curve data determining (Y_C, ξ_C) through the singularity types of C and the self-intersection number of C. In this more general setting, we find a large class of such contact structures which admit no fillings at all. In Section 6 we will define two effectively computable invariants of cuspidal singularities, M and ℓ, and we will prove a slight generalization of the following theorem.

Theorem 1.3. *Let C be a rational cuspidal curve with $\mathrm{Sing}(C) \neq \emptyset$ such that (Y_C, ξ_C) is weakly fillable. Then*

$$C \cdot C \leq \sum_{p \in \mathrm{Sing}(C)} M(p) + 2 \min_{p \in \mathrm{Sing}(C)} \ell(p) + 1.$$

Equivalently, if C is a singular rational cuspidal curve which embeds into any closed symplectic 4-manifold, the above bound on its self-intersection number holds.

Finally, we look at symplectic filling classification results in some low complexity cases. In a rational cuspidal curve C, each singularity has an underlying arithmetic genus. This can be thought of as the genus that would be added to the curve C by smoothing the cusp singularity. Adding up the arithmetic genus contributions from each singularity gives us the *arithmetic genus* of the singular curve C. To give a sample of the filling classifications for these more general examples (Y_C, ξ_C), we investigate examples where C has low arithmetic genus and varying the self-intersection $C \cdot C$ within a certain range that attains the bound of Theorem 1.3. We include these classification results in Section 7. In some cases, there is a unique minimal symplectic filling and in others there are multiple minimal symplectic fillings yielding potentially new symplectic cut-and-paste operations.

Organization. In Section 2, we give Stein handlebodies for the fillings of (Y_C, ξ_C) in the $\mathcal{A}_p$ and $\mathcal{B}_p$ cases, and prove the first two items of Theorem 1.1. Next, in Section 3, we identify (Y_C, ξ_C) with canonical contact manifolds in the $\mathcal{E}_3$ and $\mathcal{E}_6$ cases, and provide their Legendrian surgery diagrams, thus completing the proof of Theorem 1.1. In Section 4, we provide a brief summary of background from [GS22] that we will need for the remaining sections. In Section 5 we determine which fillings of (Y_C, ξ_C) are related by rational blow-downs when C is a unicuspidal curve in $\mathbb{CP}^2$, proving Theorem 1.2. Next, we look at more general examples of (Y_C, ξ_C). In Section 6, we prove Theorem 1.3. In Section 7, we give classifications of

fillings of (Y_C, ξ_C) for cases when C has small arithmetic genus. Finally, in Section 8 we provide some questions and conjectures that build off of the results we established.

Acknowledgements. Early progress on this project was made during the BIRS conference in Oaxaca *Thirty years of Floer Theory for 3-manifolds*, and the authors appreciate this excellent conference and opportunity to collaborate. We would like to thank the referee for their careful work and for their useful comments. MG acknowledges hospitality from UC Davis and LS is grateful for hospitality from Université de Nantes. We also thank Fabien Kütle and Bülent Tosun for helpful conversations related to this project. LS has been supported by NSF grants DMS 1904074 and DMS 2042345 during this project.

2. Stein handlebodies for fillings in the $\mathcal{A}_p$ and $\mathcal{B}_p$ families

Our first goal is to explicitly present Stein handlebody diagrams for the fillings of (Y_C, ξ_C) in the case that C is a rational unicuspidal curve in either the family $\mathcal{A}_p$ or $\mathcal{B}_p$. Such presentations are critical to study properties of the fillings (such as the types of surfaces they contain) and to compute their invariants. Additionally, the Stein handlebody induces a Legendrian surgery diagram for the boundary. These provide explicit ways to understand the corresponding cuspidal contact structures.

In order to verify that our Stein handlebodies have the correct contact structure on the boundary, we will use a result of Matkovič [Mat18] which classifies contact structures on Seifert fibered L-spaces in terms their underlying spin^c structure. To encode the spin^c structure concretely, we will utilize Gompf's Γ-invariant [Gom98]. Gompf provided formulas to compute this invariant for contact manifolds appearing on the boundary of a Stein handlebody in terms of the Stein handlebody diagram. We will be interested in comparing contact structures arising on the boundary of a given Stein handlebody, with the contact structures (Y_C, ξ_C) induced concavely on the boundary of a neighborhood of a rational unicuspidal curve. To facilitate this comparison, we will compute Gompf's Γ-invariant for the concavely induced structure (Y_C, ξ_C).

2.1. Gompf's Γ-invariants for rational cuspidal contact manifolds

We recall some background on spin and spin^c structures. Let $\mathrm{Fr}(Y)$ denote the $SO(3)$ bundle of oriented orthonormal frames over Y and $\mathrm{Spin}^c(3)$ be

the group $\mathrm{Spin}(3) \times \mathrm{S}^1/\{\pm 1\}$. Spin^c structures on Y are lifts of $\mathrm{Fr}(Y) \to Y$ to a $\mathrm{Spin}^c(3)$ bundle. Spin^c structures on Y are affinely in bijection with $H^2(Y;\mathbb{Z})$ through the corresponding free and transitive action, and they can be thought of as complex structures on $TY \oplus \mathbb{R}$. From [Tur02, Chapter XI.1.2], $\mathrm{Spin}^c(Y)$ is identified with the set of elements in $H^2(\mathrm{Fr}(Y);\mathbb{Z})$ whose restrictions to the $SO(3)$ fibers yield the non-zero element of $H^2(SO(3);\mathbb{Z}) = \mathbb{Z}/2\mathbb{Z}$. A choice of trivialization τ of TY gives an identification of $\mathrm{Fr}(Y)$ with $Y \times SO(3)$, and thus yields an identification of $\mathrm{Spin}^c(Y)$ with $H^2(Y;\mathbb{Z})$ (note this is not canonical as it depends on the trivialization τ).

Spin structures, on the other hand, are lifts of $\mathrm{Fr}(Y) \to Y$ to a $\mathrm{Spin}(3)$ bundle over Y, and they are canonically in bijection with trivializations of TY over the 2-skeleton of Y (with respect to a fixed cellular decomposition of Y). When Y is a rational homology 3-sphere, spin structures on Y are in bijective correspondence with self-conjugate spin^c structures on Y. To see this, following Turaev [Tur02, Chapter XI], first identify spin structures on Y with the elements of $H^1(\mathrm{Fr}(Y);\mathbb{Z}/2\mathbb{Z})$ whose restrictions to the $SO(3)$ fibers are the non-trivial element. Then the short exact sequence $\mathbb{Z} \to \mathbb{Z} \to \mathbb{Z}/2\mathbb{Z}$ induces the long exact sequence on cohomology

$$\longrightarrow H^1(\mathrm{Fr}(Y);\mathbb{Z}) \longrightarrow H^1(\mathrm{Fr}(Y);\mathbb{Z}/2\mathbb{Z}) \xrightarrow{\beta} H^2(\mathrm{Fr}(Y);\mathbb{Z}) \xrightarrow{\times 2} H^2(\mathrm{Fr}(Y);\mathbb{Z}) \longrightarrow$$

The Bockstein homomorphism $\beta : H^1(\mathrm{Fr}(Y);\mathbb{Z}/2\mathbb{Z}) \to H^2(\mathrm{Fr}(Y);\mathbb{Z})$ maps spin structures on Y to spin^c structures on Y. Since Y is a rational homology 3-sphere, $H^1(\mathrm{Fr}(Y);\mathbb{Z}) = 0$, so this map is injective. The image of the spin structures is precisely the spin^c structures $\mathfrak{s}_0$ such that $2\mathfrak{s}_0 = 0$, or equivalently $\mathfrak{s}_0 = -\mathfrak{s}_0$ (self-conjugate).

Gompf's Γ-invariant measures the 2-dimensional obstruction to uniqueness of homotopy classes of oriented 2-plane fields on a 3-manifold. Any oriented 2-plane field ξ on a 3-manifold Y determines a spin^c structure on Y (by determining a complex structure on $TY \oplus \mathbb{R}$). Gompf defines $\Gamma_\tau(\xi) \in H_1(Y;\mathbb{Z})$ to be the Poincaré dual of the class in $H^2(Y;\mathbb{Z})$ identified using τ with the spin^c structure determined by ξ. In [Gom98, Proposition 4.1], he proves various properties including that $2\Gamma_\tau(\xi)$ is Poincaré dual to $c_1(\xi)$. A trivialization τ of TY also determines a spin structure on Y (since a spin structure is a trivialization of the tangent bundle over the 2-skeleton). For each spin structure s on Y, Gompf defines an invariant $\Gamma(\xi, s) \in H_1(Y;\mathbb{Z})$. Proposition 4.8 of [Gom98] proves that if s is the spin structure determined by a trivialization τ then $\Gamma_\tau(\xi) = \Gamma(\xi, s)$ (i.e. $\Gamma_\tau(\xi)$ only depends on the spin structure induced by τ).

Let N be a standard concave neighborhood of a rational cuspidal curve C of arithmetic genus g and self-intersection $n > 0$, with boundary (Y, ξ) (we will omit the C subscripts for the rest of this section to have cleaner notation). Note, the orientation on Y *disagrees* with the boundary orientation from N. Let K denote the connected sum of the links of the singularities of C (in the $\mathcal{A}_p$ and $\mathcal{B}_p$ cases, K will be the corresponding torus knot). Then N is diffeomorphic to the knot trace $X_n(K)$ (the manifold obtained by attaching a single 2-handle to a 0-handle along K with framing n). Therefore $-Y$ has a surgery diagram consisting of the knot K with framing n. Correspondingly Y has a surgery diagram consisting of the mirror knot $m(K)$ with framing $-n$.

A spin structure on a 3-manifold with a given integral surgery diagram can be encoded by a *characteristic sublink* of the surgery diagram [Kap79] (see [GS99, Proposition 5.7.11]). Given an oriented framed link $L = L_1 \cup \cdots \cup L_\ell \subset S^3$, we let $\mathrm{lk}(L_i, L_j)$ be the linking number between L_i and L_j if $i \neq j$, and $\mathrm{lk}(L_i, L_i)$ be the framing of the component L_i (which we identify with an integer via the Seifert framing). We extend lk by bilinearity over links, so that, for instance, $\mathrm{lk}(L_i, \emptyset) = 0$. In a 3-manifold obtained by integral surgery on S^3 along a framed link L, a sublink $L' \subset L$ is *characteristic* when, for each component K_i of L, the framing of K_i is congruent modulo 2 to $\mathrm{lk}(K_i, L')$. (Note that this is insensitive to the choice of an orientation of L.) In the surgery diagram for $-Y$, which consists of a single component with framing n the only sublinks are the full link and the empty link. In the case that n is even, both of these are characteristic and there are two spin structures on $-Y$. In the case that n is odd, only the non-empty sublink is characteristic and there is a unique spin structure. In either case, let s_0 denote the spin structure on $-Y$ which corresponds to the non-empty characteristic sublink.

Theorem 2.1. *Let $(Y, \xi) = (Y_C, \xi_C)$, where C is a rational cuspidal curve of arithmetic genus g and self-intersection n. Let K be the connected sum of the links of the singularities as above. Consider the surgery diagram for $-Y$ given by n-surgery on K. Then*

$$\Gamma(\xi, s_0) = (1 - g)\mu \in H_1(-Y),$$

where s_0 is the unique spin structure on $-Y$ represented by the characteristic sublink K, and μ is the homology class represented by the meridian of K.

Proof. To set notation, we begin with some basic facts about homology and cohomology. $H_2(N; \mathbb{Z}) \cong \mathbb{Z}$ with intersection form $\langle n \rangle$ and is generated by

$[C]$. $H^2(N;\mathbb{Z}) \cong \mathbb{Z}$ and is generated by a class G where $\langle G, [C]\rangle = 1$. On the boundary, $H^2(-Y;\mathbb{Z}) \cong H_1(-Y;\mathbb{Z}) \cong \mathbb{Z}/n\mathbb{Z}$, generated by the meridian μ of the surgery knot. The restriction map $i^* : H^2(N;\mathbb{Z}) \to H^2(-Y;\mathbb{Z})$ sends G to the Poincaré dual of μ.

Since spin^c structures on a manifold M are affinely identified with $H^2(M;\mathbb{Z})$, given any two spin^c structures $\mathfrak{s}$ and $\mathfrak{s}'$ on N, their difference $\mathfrak{s}' - \mathfrak{s}$ represents a class in $H^2(N;\mathbb{Z})$. Under this identification, $c_1(\mathfrak{s}') - c_1(\mathfrak{s}) = 2(\mathfrak{s}' - \mathfrak{s})$.

We will first fix a *reference spin^c structure*, $\mathfrak{s}_0$ on N, defined by the property that

$$\langle c_1(\mathfrak{s}_0), [C]\rangle = n.$$

One important property of this reference spin^c structure is that its restriction to $\partial N = -Y$ is self-conjugate. To see this, observe that

$$\langle c_1(\bar{\mathfrak{s}}_0), [C]\rangle = -n,$$

so $\langle c_1(\mathfrak{s}_0) - c_1(\bar{\mathfrak{s}}_0), [C]\rangle = 2n$. Therefore $\mathfrak{s}_0 - \bar{\mathfrak{s}}_0 = nG \in H^2(N;\mathbb{Z})$. Then $i^*(\mathfrak{s}_0 - \bar{\mathfrak{s}}_0) = n\,\mathrm{PD}(\mu) = 0 \in H^2(-Y;\mathbb{Z})$. Therefore, $i^*(\mathfrak{s}_0)$ is self-conjugate so it corresponds to a spin structure s_0 on $-Y$.

Recall the correspondence described above between spin structures on $-Y$ and characteristic sublinks of the surgery diagram for $-Y$ given by n-surgery on K. To see that the empty sublink does not correspond to s_0 when n is even, consider the unique spin^c structure $\mathfrak{t}$ on N which satisfies $\langle c_1(\mathfrak{t}), [C]\rangle = 0$. This spin^c structure is self-conjugate on all of N, since $\mathfrak{t} - \bar{\mathfrak{t}} = 0 \in H^2(N;\mathbb{Z})$. Therefore $\mathfrak{t}$ is the image of the unique spin structure on N under the corresponding Bockstein homomorphism $\beta : H^1(\mathrm{Fr}(N);\mathbb{Z}/2\mathbb{Z}) \to H^2(\mathrm{Fr}(N);\mathbb{Z})$. Next, observe that $\langle c_1(\mathfrak{s}_0) - c_1(\mathfrak{t}), [C]\rangle = n$, so $\mathfrak{s}_0 - \mathfrak{t} = \frac{n}{2}G \in H^2(N;\mathbb{Z})$, and the restriction to $-Y$, $i^*(\mathfrak{s}_0 - \mathfrak{t}) = \frac{n}{2}\,\mathrm{PD}(\mu) \in H^2(-Y;\mathbb{Z})$. Since $\frac{n}{2}\,\mathrm{PD}(\mu)$ is a non-zero element in $H^2(-Y;\mathbb{Z})$, $i^*(\mathfrak{s}_0) \neq i^*(\mathfrak{t})$. Therefore these two self-conjugate spin^c structures on $-Y$ correspond to distinct spin structures on $-Y$. Since $i^*(\mathfrak{t})$ corresponds to the empty sublink (by definition, the empty sublink of an integral surgery diagram corresponds to the spin structure which extends over the corresponding 4-manifold described as that 2-handlebody), s_0 must correspond to the non-empty sublink.

Now, we consider two spin^c structures on N, our reference spin^c structure $\mathfrak{s}_0$ and the spin^c structure $\mathfrak{s}_J$, coming from an almost complex structure on N compatible with the symplectic structure, such that the complex tangencies of J along Y give the contact structure ξ. The difference of these two spin^c structures corresponds to a class $\mathfrak{s}_J - \mathfrak{s}_0 \in H^2(N;\mathbb{Z})$. We know that

$2(\mathfrak{s}_J - \mathfrak{s}_0) = c_1(\mathfrak{s}_J) - c_1(\mathfrak{s}_0)$, so since $H^2(N;\mathbb{Z}) \cong \mathbb{Z}$ has no 2-torsion, we can determine the class $\mathfrak{s}_J - \mathfrak{s}_0$ uniquely from computing the Chern classes.

By definition, we chose $\mathfrak{s}_0$ to have $c_1(\mathfrak{s}_0) = nG$ (where G is the generator dual to $[C]$). We can use the adjunction formula to compute

$$\langle c_1(\mathfrak{s}_J), [C] \rangle = 2 - 2g + n.$$

(This can be seen by replacing C by a curve which smooths its singularities symplectically, thus increasing the genus of C to its arithmetic genus without changing the homology class it represents. This symplectic smoothing procedure is surgical and local in nature: any curve singularity in $\mathbb{C}^2$ and its Milnor fiber have the same link, as transverse knots, and so we can remove the former and glue in the latter symplectically to get rid of one singularity of a curve.)

Therefore $c_1(\mathfrak{s}_J) - c_1(\mathfrak{s}_0) = (2 - 2g + n - n)[G]$, so

$$\mathfrak{s}_J - \mathfrak{s}_0 = (1-g)G \in H^2(N;\mathbb{Z}).$$

Restricting this class to the boundary, $\partial N = -Y$, we have $i^*(\mathfrak{s}_J) - i^*(\mathfrak{s}_0) = (1-g)\,\mathrm{PD}(\mu)$.

Now recall the definition of $\Gamma(\xi, s_0)$ from the beginning of this subsection. Since ξ is given by the complex tangencies to $-Y$ under the almost complex structure J, $\mathfrak{s}_J$ restricts to the spin^c structure on $-Y$ determined by ξ. If τ is a trivialization that induces the spin structure s_0, then $\Gamma(\xi, s_0)$ is the Poincaré dual to the class in $H^2(-Y;\mathbb{Z})$ corresponding to the spin^c structure $i^*(\mathfrak{s}_J)$ (where the correspondence depends on τ). Note that under this correspondence the spin^c structure $i^*(\mathfrak{s}_0)$ corresponds to the 0 element in $H^2(-Y;\mathbb{Z})$. Therefore, $\Gamma(\xi, s_0) = \mathrm{PD}(i^*(\mathfrak{s}_J) - i^*(\mathfrak{s}_0))$, and the result follows. □

2.2. Stein handlebodies for fillings

Observe that any symplectic filling of (Y_C, ξ_C) can be capped by a concave neighborhood of the cuspidal curve C to form a closed symplectic manifold. Equivalently, every symplectic filling of (Y_C, ξ_C) arises as the complement of a neighborhood of a symplectic embedding of C into a closed symplectic manifold. When C is a rational and unicuspidal curve in $\mathbb{CP}^2$, we classify such embeddings in [GS22, Theorem 6.5]. The goal of this section is to turn this perspective upside down, by translating our understanding of the embedding of C into a concrete description of the Stein domain in its complement.

For smooth handle decompositions, we can literally turn handle diagrams upside down (negating the Morse function) to obtain handle decompositions for many complements. However, it is not clear that a given smooth handle decomposition for a complement will support a Stein structure. Since there is not a notion of symplectic handle attachment for closed 4-manifolds, the strategy of turning things upside down does not suffice to identify a Stein handle structure on the complement, so we will use additional arguments to show we have identified the correct geometric structure.

We start with the case where C is in the family $\mathcal{A}_p$. In this case C has a unique singularity whose link is $T(p, p+1)$ so its arithmetic genus is $\frac{p(p-1)}{2}$. The self-intersection number is $(p+1)^2$. Then [GS22, Theorem 6.5] tells us that the only minimal symplectic embedding of C into a closed symplectic manifold is into $\mathbb{CP}^2$ and that there is a unique symplectic isotopy class of such an embedding. As a consequence (Y_C, ξ_C) has a unique minimal symplectic filling, which is diffeomorphic to an affine complex surface after attaching a cylindrical end. Our aim is to give a Stein handlebody description of this object.

Theorem 2.2. *Fix $p > 1$, and let C be a curve of type $\mathcal{A}_p$. Then the unique filling of (Y_C, ξ_C) is the Stein handlebody W_{hb} given by the diagram in Figure 1 (up to symplectic deformation and symplectomorphism).*

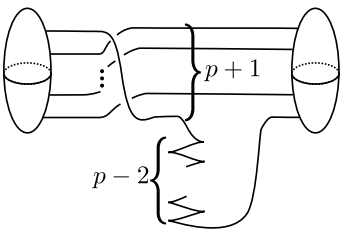

Figure 1. Stein handlebody for the filling corresponding to the $\mathcal{A}_p$ family. The framing on the 2-handle is $tb - 1 = 1$.

That the filling has a handle decomposition with only one 1-handle and one 2-handle was to be expected from the proof of [GS22, Theorem 6.5]. Indeed, in that proof we show that, letting T be the tangent to the cusp of C, the configuration $C \cup T$ is birationally equivalent to the configuration of two lines in $\mathbb{CP}^2$, and in particular its complement is diffeomorphic to $S^1 \times D^3$. The handle decomposition corresponding to adding a neighborhood of $T \setminus C$

corresponds to attaching a 2-handle. In fact, using this argument one obtains the (smooth) Kirby diagram underlying Figure 1.

Proof. To simplify notation, we will write (Y, ξ) instead of (Y_C, ξ_C). Since Y is the boundary of a neighborhood of the rational cuspidal curve of type $\mathcal{A}_p$ (with the orientation reversed), $Y = -S^3_{(p+1)^2}(T(p, p+1))$. It follows, for instance from [OS12, Lemma 4.4], that Y is a small Seifert fibered space with Seifert invariants $(-1; \frac{p}{p+1}, \frac{1}{p}, \frac{1}{p+1})$ (see Figure 8 for the Seifert fibered notation).

Since $(p^2 + p + 1)$-surgery along $T(p, p+1)$ is a lens space [Mos71], the torus knot $T(p, p+1)$ is an L-space knot. Since $(p+1)^2 \geq 2g(T(p, p+1)) - 1$, by [LS04, Proposition 4.1] Y is a Heegaard Floer L-space.

Matkovič proved in [Mat18, Theorem 1.3] that two tight contact structures on a small Seifert fibered L-space are isotopic if and only if they induce the same spin^c structure. We will compute Gompf's Γ-invariant (with respect to the same spin structure on Y) for the contact structure ξ_{hb} described by the Stein handlebody of Figure 1 and use Theorem 2.1 to say that $\Gamma(\xi, s_0) = \Gamma(\xi_{\text{hb}}, s_0)$; that is, ξ_{hb} and ξ induce the same spin^c structure. Since both ξ_{hb} and ξ are tight, by Matkovič's result they are isotopic. Note that when $p+1$ is odd computing the first Chern class of ξ_{hb} and ξ would suffice. However, when $p+1$ is even, $H_1(Y)$ contains 2-torsion, so knowing that the first Chern classes agree does not suffice to prove that the spin^c structures are the same.

We have one surgery presentation, P_0, for $-Y$ given by $(p+1)^2$-surgery on $T(p, p+1)$. In order to compare Γ-invariants, we need to relate this to the surgery diagram for Y given as the boundary of W_{hb}. Note that in order to obtain a surgery diagram for Y from the handle diagram for W_{hb} of Figure 1, we need to switch to dotted circle notation for the 1-handle, and then replace the dotted circle with a 0-framed circle. The resulting diagram represents a smooth 4-manifold W^*_{hb} obtained by surgering out the $S^1 \times D^3$ going around the 1-handle and replacing it by $S^2 \times D^2$, but its boundary is unchanged. We will refer to this surgery diagram for Y as P_1, and will denote its two components by K_0 and K_1 where K_0 is 0-framed and K_1 is $+1$-framed. (To see the framing on K_1 from Figure 1, calculate $\text{tb} - 1$ using [Gom98, Equation (1.1)], using the framing convention of [Gom98, page 634].)

To relate P_0 and P_1, we first reverse the orientation of P_0, and then perform a sequence of Kirby calculus moves as in Figure 2, in which (a) is P_0 and (b) is obtained from (a) by reversing the orientation. To go from (b) to (c) we perform an anti-blow-up, which introduces a $+1$-framed unknot

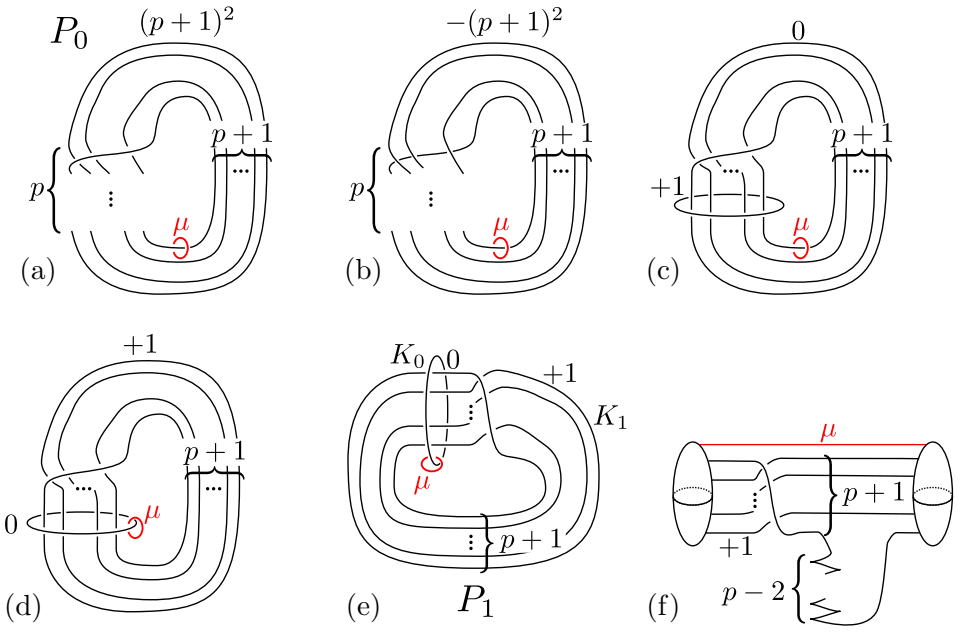

Figure 2. Kirby calculus moves relating surgery presentation P_0 to surgery presentation P_1, where the surgery presentation P_1 is induced by the Stein handlebody in the bottom right.

and adds a full positive twist into the strands of the mirror of $T(p, p+1)$ and changes its framing to 0. This results in a symmetric link, so there is an isotopy which exchanges the two components, taking us to (d). (e) is isotopic to (d), and to obtain the final surgery presentation P_1 in (f), we do a zero-dot surgery, which replaces a 0-framed 2-sphere with a 1-handle. This sequence of Kirby calculus moves provides an explicit diffeomorphism identifying the two surgery presentations. We can carry the curve in Y given by the meridian μ of $T(p, p+1)$ through the Kirby calculus moves to see its image under this diffeomorphism. Following Figure 2, we see that μ is sent to the meridian of K_0 in the surgery presentation P_1, or equivalently a curve which passes once through the 1-handle in the boundary of W_{hb}.

In the statement of Theorem 2.1, the spin structure s_0 is represented in the surgery presentation P_0 by the non-empty characteristic sublink, i.e. $T(p, p+1)$. We would like to identify this characteristic sublink in the surgery presentation P_0 with a characteristic sublink of the surgery presentation P_1. Note that, when $p+1$ is odd, there is a unique characteristic

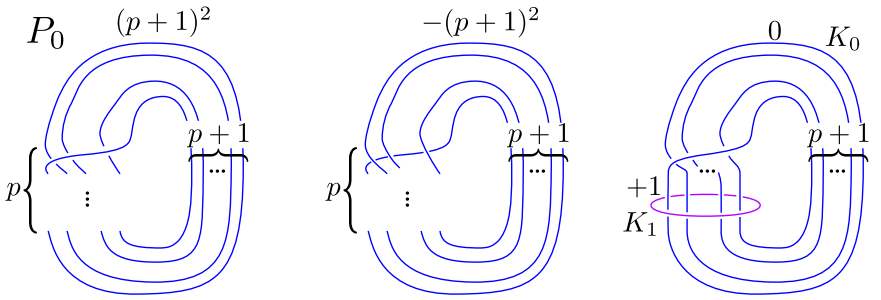

Figure 3. The characteristic sublink in P_0 represented by the colored $T(p+1,p)$ is carried through the Kirby calculus moves. Reversing orientation keeps the same component in the characteristic sublink. The anti-blow-up adds the $+1$-framed component K_1 to the characteristic sublink if and only if $\mathrm{lk}(K_1,K_0)=p+1$ is even.

sublink K_0 in the surgery diagram P_1. When $p+1$ is even, there are two characteristic sublinks of P_1: K_1 and $K_0\cup K_1$, so we need to determine which of these corresponds to s_0. It is explained in [GS99, Pages 190–191] how to track the characteristic sublink through Kirby calculus moves, and specifically through a blow-up. The characteristic sublink during a blow-up is unchanged except that the new $+1$-framed unknotted component is included if and only if it has even linking number with the previous characteristic sublink. Therefore, after we push s_0 through the Kirby calculus moves, it is represented by the sublink $K_0\cup K_1$ when $p+1$ is even, and by K_0 when $p+1$ is odd. See Figure 3.

Given a Stein handlebody diagram in standard form, Gompf provides a formula to determine the Γ-invariant for the contact structure induced on the boundary. Let ξ_{hb} denote the contact structure induced on the boundary of the Stein handlebody W_{hb}. Recall that P_1 is a handlebody diagram for a 4-manifold W^*_{hb} obtained by surgering W_{hb}. The 2-handles attached to K_0 and K_1 determine homology classes α_0 and α_1 respectively which form a basis for $H_2(W^*_{\mathrm{hb}};\mathbb{Z})$ (α_i is represented by a surface obtained by capping off a Seifert surface for K_i). By [Gom98, Theorem 4.12], $\Gamma(\xi_{\mathrm{hb}},s_0)$ is Poincaré dual to the cohomology class $j^*\rho\in H^2(Y;\mathbb{Z})$, where $j\colon Y\to W^*_{\mathrm{hb}}$ is the inclusion

and $\rho \in H^2(W^*_{\mathrm{hb}};\mathbb{Z})$ satisfies:

$$\text{(2.1)} \qquad \begin{cases} \langle \rho, \alpha_0 \rangle = \frac{1}{2}\,\mathrm{lk}(K_0, L' + K_0), \\ \langle \rho, \alpha_1 \rangle = \frac{1}{2}\left(\mathrm{rot}(K_1) + \mathrm{lk}(K_1, L' + K_0)\right), \end{cases}$$

where L' is the characteristic sublink of W^*_{hb} corresponding to s_0 (namely if $p+1$ is odd $L' = K_0$ and if $p+1$ is even $L' = K_0 \cup K_1$). Note that, as observed in [Gom98, Section 4], the link $L' + K_0$ is to be interpreted modulo 2; in particular, if $K_0 \subset L'$ then $L' + K_0 = L' \setminus K_0$.

$H^2(W^*_{\mathrm{hb}};\mathbb{Z})$ is Poincaré dual to $H_2(W^*_{\mathrm{hb}}, Y;\mathbb{Z})$, which is generated by the classes of the meridian disks D_0 and D_1 to K_0 and K_1, respectively. Since $\langle \rho, \alpha_i \rangle = \mathrm{PD}(\rho) \cdot \alpha_i$, and D_i is a geometric dual of α_i, we have that

$$\mathrm{PD}(\rho) = \frac{1}{2}\,\mathrm{lk}(K_0, L' + K_0)[D_0] + \frac{1}{2}\left(\mathrm{rot}(K_1) + \mathrm{lk}(K_1, L' + K_0)\right)[D_1].$$

We also have that $\mathrm{PD}(j^*(\rho)) = \partial(\mathrm{PD}(\rho))$ as in the following commutative diagram:

$$\begin{array}{ccc} H^2(W^*_{\mathrm{hb}};\mathbb{Z}) & \xrightarrow{j^*} & H^2(Y;\mathbb{Z}) \\ \big\downarrow \mathrm{PD} & & \big\downarrow \mathrm{PD} \\ H_2(W^*_{\mathrm{hb}}, Y;\mathbb{Z}) & \xrightarrow{\partial} & H_1(Y;\mathbb{Z}) \end{array}$$

The boundary map $\partial\colon H_2(W^*_{\mathrm{hb}}, Y;\mathbb{Z}) \to H_1(Y;\mathbb{Z})$ sends $[D_0]$ to $[\partial D_0] = \mu \in H_1(Y;\mathbb{Z})$. Using the fact that a presentation of $H_1(Y;\mathbb{Z})$ can be obtained from the surgery diagram P_1, with generators $[\partial D_0]$ and $[\partial D_1]$ and relations presented by the intersection matrix $\left(\begin{smallmatrix} 0 & p+1 \\ p+1 & 1 \end{smallmatrix}\right)$, we see that

$$[\partial D_1] = -(p+1)[\partial D_0] = -(p+1)\mu \quad \text{and} \quad (p+1)^2\mu = 0.$$

Therefore

$$\begin{aligned} \Gamma(\xi_{\mathrm{hb}}, s_0) &= \mathrm{PD}(j^*\rho) = \partial\,\mathrm{PD}(\rho) \\ &= \frac{1}{2}\,\mathrm{lk}(K_0, L' + K_0)[\partial D_0] + \frac{1}{2}\left(\mathrm{rot}(K_1) + \mathrm{lk}(K_1, L' + K_0)\right)[\partial D_1] \\ &= \frac{1}{2}\left(\mathrm{lk}(K_0, L' + K_0) - (p+1)\left(\mathrm{rot}(K_1) + \mathrm{lk}(K_1, L' + K_0)\right)\right)\mu. \end{aligned}$$

Finally, by counting the number of downward cusps minus the number of upward cusps in the Stein handlebody diagram of Figure 1, we see that $\mathrm{rot}(K_1) = p - 2$.

Let us now look at the two cases, according to the parity of $p+1$.

If $p+1$ is odd, $L' = K_0$, so we can take the empty link as a mod 2 representative of $L' + K_0$. Therefore,

$$\begin{aligned}\Gamma(\xi_{\mathrm{hb}}, s_0) &= \frac{1}{2}\left(\mathrm{lk}(K_0, \emptyset) - (p+1)\left(\mathrm{rot}(K_1) + \mathrm{lk}(K_1, \emptyset)\right)\right)\mu \\ &= -\frac{(p+1)(p-2)}{2}\mu = \frac{-p^2+p+2}{2}\mu.\end{aligned}$$

If $p+1$ is even $L' = K_0 \cup K_1$, so we can take K_1 as a mod 2 representative of $L' + K_0$. Therefore,

$$\begin{aligned}\Gamma(\xi_{\mathrm{hb}}, s_0) &= \frac{1}{2}\left(\mathrm{lk}(K_0, K_1) - (p+1)\left(\mathrm{rot}(K_1) + \mathrm{lk}(K_1, K_1)\right)\right)\mu \\ &= \frac{p+1-(p+1)(p-2+1)}{2}\mu = \frac{-p^2+p+2}{2}\mu.\end{aligned}$$

Comparing this with the calculation from Proposition 2.1 with $g = \frac{p(p-1)}{2}$ (the arithmetic genus of the singularity with link $T(p, p+1)$), we see that

$$\Gamma(\xi, s_0) = \left(1 - \frac{p(p-1)}{2}\right)\mu = \frac{-p^2+p+2}{2}\mu = \Gamma(\xi_{\mathrm{hb}}, s_0).$$

Therefore, by Matkovič's result, ξ and ξ_{hb} are contactomorphic. Since ξ has a unique minimal symplectic filling, W_{hb} must be this filling (up to symplectic deformation and symplectomorphism). □

For symplectic curves in the $\mathcal{B}_p$ family, we prove in [GS22, Theorem 6.5], that there are exactly two relatively minimal symplectic embeddings of C into closed symplectic manifolds up to symplectic isotopy: one embedding is into $\mathbb{CP}^2$ and the other is into $S^2 \times S^2$. Consequently, there are exactly two minimal symplectic fillings of (Y_C, ξ_C) (up to symplectic deformation and symplectomorphism): one is a rational homology ball and the other has $b_2 = 1$.

Theorem 2.3. *Fix $p > 1$, and let C be the rational cuspidal curve of type $\mathcal{B}_p$. Then the unique rational homology ball filling of (Y_C, ξ_C) is given by the Stein handlebody depicted in Figure 4, and the unique filling of (Y_C, ξ_C) with $b_2 = 1$ is given by the Stein handlebody of Figure 5.*

The proof will follow the same method as Theorem 2.2. A heuristic argument, similar to that we gave for the $\mathcal{A}_p$ family, for why the filling has a

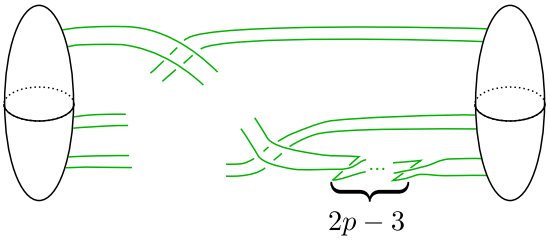

Figure 4. Stein handlebody diagram for the rational homology ball filling of (Y_C, ξ_C) where C is a $\mathcal{B}_p$-type rational unicuspidal curve. The attaching curve for the 2-handle passes through the 1-handle $2p$ times. Observe that for the Legendrian attaching curve for the 2-handle, $\mathrm{tb} = 4(p-1) - (2p-3) - (2p-3) = 2$ and $\mathrm{rot} = 2p - 3$.

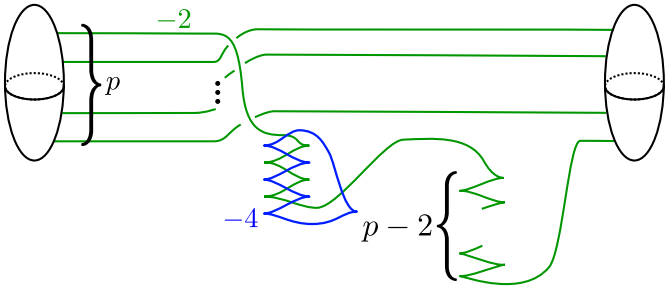

Figure 5. Stein handlebody diagram for the $b_2 = 1$ filling of (Y_C, ξ_C) where C is a $\mathcal{B}_p$-type rational unicuspidal curve. Observe that the blue Legendrian attaching curve has $\mathrm{tb} = -1$ and $\mathrm{rot} = p$, and the green Legendrian attaching curve has $\mathrm{tb} = -3$ and $\mathrm{rot} = 2$.

decomposition with one 1-handle and one 2-handle is found by considering $C \cup T$, where T is the tangent to C at the cusp.

Proof. The boundary of the handlebody is Y_C as seen by the sequence of Kirby calculus moves in Figure 6, which are explained in the caption. The isotopy from the bottom left diagram to the bottom right one can be thought of in terms of the following observation. As a link, the diagram on the bottom left is the obtained from the Hopf link by taking the $(2,1)$-cable of one component and the $(p,1)$-cable of the other. Since the link obtained

by doing the $(p,1)$-cable on the Hopf link is symmetric, we can choose to "discharge" the cabling on the first component, so that cabling the two components separately is the same as cabling one component twice. One needs to keep track of the framing, using the writhe, to see that there are $(p-1)$ negative twists.

We also track the class μ and the spin structure s_0 (represented by the non-empty characteristic sublink) through these diagrams. Since the (green) $+1$-unknot of the blow-up links the (black) knotted component $2p$ times, by [GS99, Pages 190–191], the $+1$-framed unknot is included in the characteristic sublink corresponding to s_0. That is, in the last diagram the spin structure s_0 is represented by the characteristic sublink consisting of *both* components of the surgery diagram.

Since the $\mathcal{B}_p$ curve has arithmetic genus $\frac{(p-1)(4p-2)}{2}$, using Theorem 2.1, we see that

$$\Gamma(\xi_C, s_0) = (1-(p-1)(2p-1))\mu = (3p-2p^2)\mu.$$

Let ξ_{hb} be the contact structure represented by the Legendrian surgery diagram of Figure 4. We compare $\Gamma(\xi_C, s_0)$ and $\Gamma(\xi_{\mathrm{hb}}, s_0)$, following the same computation as in the $\mathcal{A}_p$ case.

As in the proof of Theorem 2.2, call W^*_{hb} the surgery diagram on the top right of Figure 6 (i.e. the one obtained from doing a zero-dot surgery on W_{hb}), and call K_0 and K_1 the components of the link, where K_0 is the 0-framed component (black) and K_1 is the 1-framed component. With a slight abuse of notation, we also call K_1 the Legendrian attaching curve of Figure 4, which we orient as going from left to right. We orient K_0 so that $\mathrm{lk}(K_0, K_1) = 2p$. Once again, we use the conventions from [Gom98] to compute Thurston–Bennequin and rotation numbers in the presence of 1-handles.

Using these conventions, we compute the classical invariants of K_1. There are $4(p-1)$ positive crossings coming from the $1/p^{\mathrm{th}}$ of twist on the left, $2p-3$ negative crossings coming from the 2-cabling on the right, and $4p-6$ cusps, all of which are downward-pointing. Summing up:

$$\begin{aligned} \mathrm{tb}(K_1) &= 4(p-1) - (2p-3) - (2p-3) = 2; \\ \mathrm{rot}(K_1) &= \tfrac{4p-6}{2} = 2p-3. \end{aligned}$$

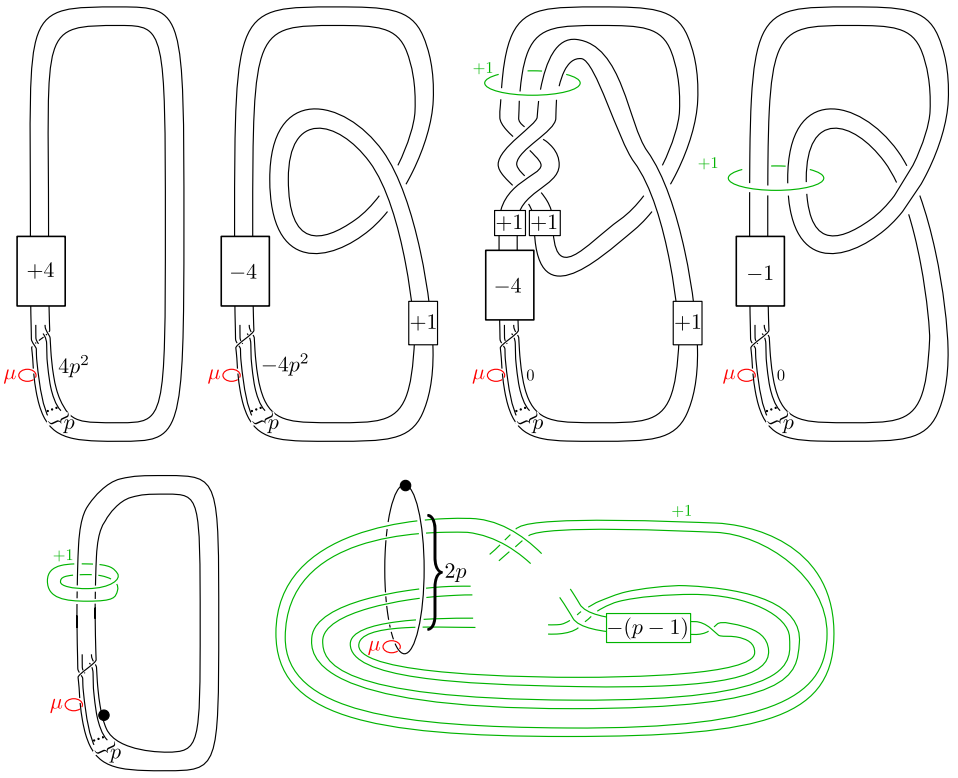

Figure 6. A Kirby calculus sequence from the surgery presentation of Y to a rational homology ball. Along the top, going from the left most figure to the next corresponds to reversing orientation and performing an isotopy, then the next figure is related by an anti-blow-up, and the rightmost is related by an isotopy. The bottom left figure is related by an isotopy and switching the 0-framed component to a dotted circle, and the bottom right figure is obtained by an isotopy to put it in standard notation. This bottom right figure is the same underlying smooth handlebody diagram as Figure 4 (the signed number of crossings between the two strands at the bottom is $-2(p-1)+1 = -(2p-3)$, and the framing $+1 = \mathrm{tb}\,-1$ for the Legendrian realization in Figure 4).

Note that $\mathrm{tb}(K_1) - 1 = +1$, so that the framing coming from the Legendrian surgery picture of Figure 4 agrees with the smooth surgery framing of Figure 6.

Call D_0 and D_1 the co-cores of the handles associated to the surgeries along K_0 and K_1, respectively. The intersection matrix of W_{hb}^* is $\left(\begin{smallmatrix} 0 & 2p \\ 2p & 1 \end{smallmatrix}\right)$, so we have $[\partial D_0] = \mu \in H_1(Y)$ and $[\partial D_1] = -2p\mu \in H_1(Y)$.

Recall that s_0 corresponds to the characteristic sublink $L' := K_0 \cup K_1$ containing both components of the link in Figure 6. The same computation as in the proof of Theorem 2.2 now yields:

$$\begin{aligned}
\Gamma(\xi_{\mathrm{hb}}, s_0) &= \mathrm{PD}(j^*\rho) = \partial\,\mathrm{PD}(\rho) \\
&= \frac{1}{2}\,\mathrm{lk}(K_0, L' + K_0)[\partial D_0] + \frac{1}{2}\left(\mathrm{rot}(K_1) + \mathrm{lk}(K_1, L' + K_0)\right)[\partial D_1] \\
&= \frac{1}{2}\,\mathrm{lk}(K_0, K_1)\mu + \frac{1}{2}(\mathrm{rot}(K_1) + \mathrm{lk}(K_1, K_1))(-2p)\mu \\
&= p\mu - p(2p - 3 + 1)\mu \\
&= (3p - 2p^2)\mu.
\end{aligned}$$

Therefore, we have that $\Gamma(\xi_{\mathrm{hb}}, s_0) = \Gamma(\xi, s_0)$. That is, ξ_{hb} and ξ induce the same spin^c structure on Y. Now, $-Y$ is obtained as $4p^2$-surgery along $T(p, 4p-1)$, so Y is a small Seifert fibered space. Moreover, since $4p^2 > 2g(T(p, 4p-1)) - 2$, by [LS04, Proposition 4.1] Y is a also a Heegaard Floer L-space. Since both ξ and ξ_{hb} are tight, Matkovič's result [Mat18, Theorem 1.3] implies that ξ_{hb} and ξ are isotopic.

For the filling with $b_2 = 1$, the proof goes similarly, comparing the Γ-invariant calculation for the Stein handlebody of Figure 5 with that of Theorem 2.1. We leave this computation to the reader, but provide assistance with Figure 7, which gives a Kirby calculus sequence between the surgery diagram for Y_C as $-S^3_{4p^2}(T(p, 4p-1))$ and one which is equivalent to Figure 5 by an isotopy plus surgering a 0-framed 2-handle to a 1-handle. □

3. Canonical contact structures in the exceptional $\mathcal{E}_3$ and $\mathcal{E}_6$ cases

In this section, we focus on (Y_C, ξ_C) for the two exceptional cases of rational cuspidal curves in $\mathbb{CP}^2$ with a single $T(a, b)$ cusp, with $(a, b) = (3, 22)$ or $(a, b) = (6, 43)$. Our goal is to identify the contact manifolds in these two cases as the canonical contact manifolds arising as links of complex normal surface singularities. This will complete the proof of Theorem 1.1.

In the proofs, we will make use of the Ozsváth–Szabó contact invariant [OSz05] in Heegaard Floer homology [OSz04]. The relevant properties

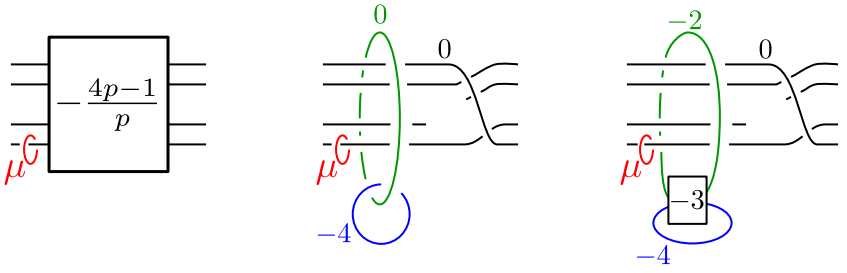

Figure 7. An abbreviated Kirby calculus sequence for Y_C in the $\mathcal{B}_p$ case to help compare the Γ-invariant for the second filling. The right most diagram can be isotoped so that after exchanging the 0-framed 2-handle for a dotted circle and switching to the other 1-handle notation, we get a diagram which is smoothly equivalent to Figure 5. To get from the center figure to the left, handle slide all p strands the black curve over the blue curve, and then cancel the blue and green curves. To get from the center figure to the right, handle slide the green curve once over the blue curve. The spin structure represented by the non-empty characteristic sublink on the left corresponds to the spin structure represented by the characteristic sublink in the center and right diagrams which consists of the black component only when p is even, and the black and blue components when p is odd.

of the theory are the non-vanishing of the contact invariant for fillable contact structures [OSz05, Theorem 1.5], the fact that large surgeries on torus knots are L-spaces (i.e. they have the smallest possible Heegaard Floer homology) [LS04, Proposition 4.1], and the absolute grading on Heegaard Floer homology [OSz03].

We first consider the contact 3-manifold (Y_C, ξ_C) associated to the curve $\mathcal{E}_3$, which is associated to the triple $(3, 22; 8)$. Then topologically, $Y_C = -S^3_{64}(T(3, 22))$. In particular, it is a small Seifert fibered manifolds with Seifert parameters $(-2; 1/2, 1/3, 15/22)$; see Figure 8 for an explanation of the notation.

Expanding the rational surgeries with their continued fraction expansions, we see that Y_C is smoothly the boundary of the following plumbing

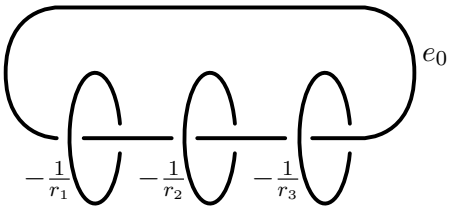

Figure 8. A surgery description for the small Seifert fibered manifold with parameters $(e_0; r_1, r_2, r_3)$.

graph.

(3.1)

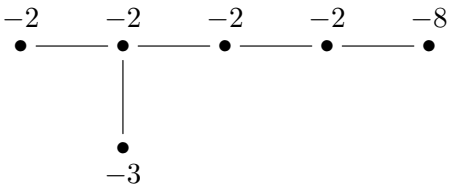

The *canonical* contact structure of a Seifert fibered space is the one arising as convex boundary of a plumbing of symplectic spheres according to a negative definite graph. Equivalently, it is the contact structure that arises as the link of a complex surface singularity whose minimal normal crossing resolution is that plumbing. Note that the graph (3.1) does have a negative definite intersection form.

Proposition 3.1. *When C is the rational cuspidal curve with a single $T(3, 22)$ cusp and self-intersection number 64, the contact manifold (Y_C, ξ_C) is contactomorphic to the canonical contact structure on Y_C associated with the plumbing* (3.1)*. It can be presented as a Legendrian surgery diagram as in Figure 9.*

Proof. Tosun [Tos20, Theorem 1.1(b)] classified tight contact structures on small Seifert fibered spaces with $e_0 = -2$ and $r_1 + r_2 + r_3 < 2$, showing that all such tight contact structures all arise from a Legendrian surgery picture associated to the plumbing (3.1), as in Figure 10. Since (Y_C, ξ_C) is fillable, ξ_C is tight [EG91]. As explained above Y_C is the small Seifert fibered space with $(e_0; r_1, r_2, r_3) = (-2; 1/2, 1/3, 15/22)$. Since, $r_1 + r_2 + r_3 = \frac{50}{33} < 2$, Tosun's classification result applies.

We will prove that the canonical contact structure is the unique tight contact structure (on the Seifert fibered space at hand) whose associated

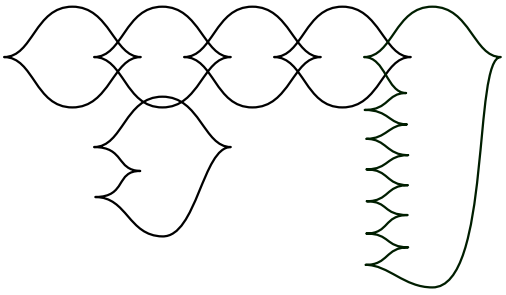

Figure 9. Stein handlebody for the plumbing inducing the canonical contact structure on its boundary.

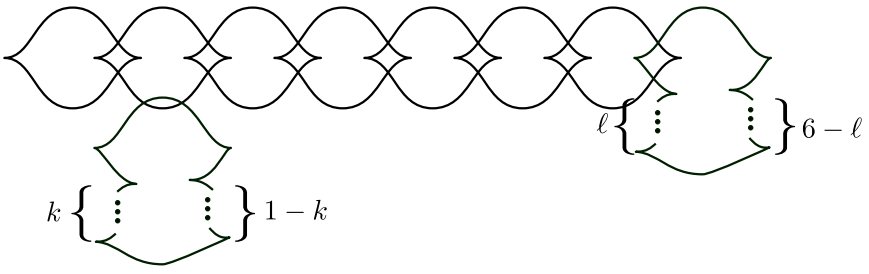

Figure 10. Allowing some number of the stabilizations of unknotted components of Figure 9 to be negative provides Legendrian surgery diagrams for all other tight contact structures on this 3-manifold by a result of Tosun.

spin^c structure $\mathfrak{t}$ extends to a rational homology ball. We do this by computing the Heegaard Floer correction term associated to the spin^c classes of all tight contact structures, using Tosun's classification.

We begin by observing that, since (Y_C, ξ_C) has a rational homology ball filling, then the correction term $d(Y_C, \mathfrak{t})$ vanishes. We set out to prove that this characterises the canonical contact structure (up to conjugation).

Since torus knots are L-space knots (in fact, lens space knots [Mos71]), and the surgery coefficient is 64, which is larger than $2g(T(3,22)) - 2 = 40$, Y is an L-space [LS04, Proposition 4.1]. (Now we could use Ghiggini's classification result from [Ghi08] instead of Tosun's, as mentioned in the introduction.)

Since every tight contact structure on Y_C arises as the boundary of a Stein handlebody as in Figure 10, we can use this Stein filling to compute the

degree of the contact invariant for each contact structure. The contact invariant is also the generator of the associated tower in $\mathrm{HF}^+(Y)$, so its degree is the correction term associated to the corresponding contact structure.

The possible realizations of the link L are distinguished by the rotation numbers s, t of the components with framing -3 and -8: these can take values ± 1 and ± 6, ± 4, ± 2, or 0, respectively. All other rotation numbers vanish, since the framing is -2. Moreover, reversing both signs corresponds to conjugation. Let $J_{s,t}$ be the complex structure on the Stein plumbing P associated to Legendrian realization of the link with rotation numbers s and t, and $\xi_{s,t}$ the associated contact structure on Y_C.

Since $c_1(J_{s,t})$ evaluates on a sphere in the plumbing as the rotation number of the corresponding unlink, we can compute $c_1^2(J_{s,t})$ from the intersection matrix Q of the plumbing P. Q and its inverse Q^{-1} are:

$$Q = \begin{pmatrix} -2 & 1 & 1 & 1 & 0 & 0 \\ 1 & -2 & 0 & 0 & 0 & 0 \\ 1 & 0 & -3 & 0 & 0 & 0 \\ 1 & 0 & 0 & -2 & 1 & 0 \\ 0 & 0 & 0 & 1 & -2 & 1 \\ 0 & 0 & 0 & 0 & 1 & -8 \end{pmatrix},$$

$$Q^{-1} = -\frac{1}{64} \begin{pmatrix} 132 & 66 & 44 & 90 & 48 & 6 \\ 66 & 65 & 22 & 45 & 24 & 3 \\ 44 & 22 & 36 & 30 & 16 & 2 \\ 90 & 45 & 30 & 105 & 56 & 7 \\ 48 & 24 & 16 & 56 & 64 & 8 \\ 6 & 3 & 2 & 7 & 8 & 9 \end{pmatrix}.$$

Then $c_1^2(J_{s,t}) = vQ^{-1}v^t$, where $v = (0, 0, s, 0, 0, t)$.

For convenience, call $P^* = P \setminus B^4$, a cobordism from S^3 to Y. Then,

$$\frac{c_1^2(J_{s,t}) - 2\chi(P^*) - 3\sigma(P^*)}{4} = \frac{384 - 36s^2 - 4st - 9t^2}{256},$$

and it is easily verified that the minimum of this function, with $s = \pm 1$ and $t \in \{0, \pm 2, \pm 4, \pm 6\}$ is 0, attained only at $(s, t) = \pm(1, 6)$; that is, only at the canonical contact structure and its conjugate. □

Remark 3.2. We note that when understanding symplectic fillings, identifying a contact structure up to contactomorphism and conjugation suffices. This is because, for every symplectic filling of a contact manifold, the same filling with the conjugate almost complex structure (negating the symplectic

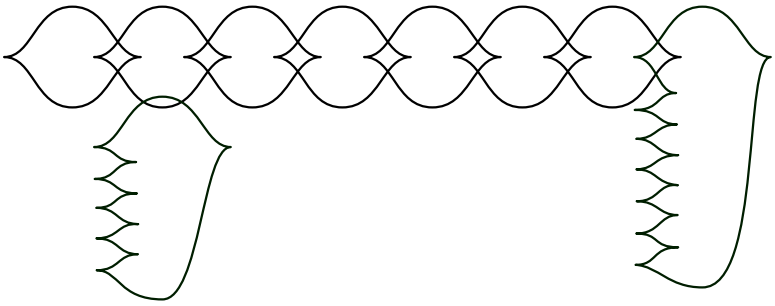

Figure 11. Stein handlebody for the plumbing inducing the canonical contact structure on its boundary.

form) gives a symplectic filling of the conjugate contact manifold. Therefore the fillings of a contact manifold and its conjugate are in bijective correspondence.

Next, we consider the second exceptional case, where C has a unique singularity of type $(6, 43)$ and self-intersection number $16^2 = 256$. In this case, $Y_C = -S^3_{256}(T(6, 43))$, so Y_C is a small Seifert fibered space with Seifert parameters $(-2; 1/2, 1/6, 36/43)$. A negative definite plumbing with boundary Y_C is the following.

(3.2)

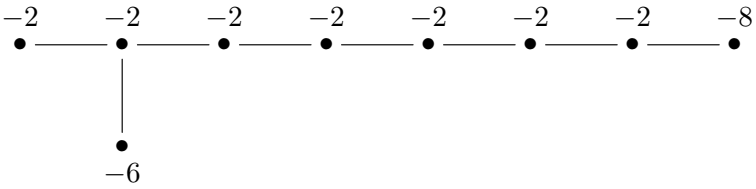

Proposition 3.3. *When C is the rational cuspidal curve with a single $T(6, 43)$ cusp and self-intersection number 256, the contact manifold (Y_C, ξ_C) is contactomorphic to the canonical contact structure on Y_C associated with the plumbing* (3.2)*. It can be presented as a Legendrian surgery diagram as in Figure 11.*

Proof. Since the proof is very similar to that of Proposition 3.1, we omit the details that would be repeated and only include the calculations where the two cases differ.

Again, in this case we have $r_1 + r_2 + r_3 = \frac{194}{129} < 2$, so Tosun's classification result still applies. Moreover, the surgery coefficient is again sufficiently large, so Y_C is again an L-space.

In the plumbing graph there are still only two rotation numbers s and t that vary, corresponding to the vertices of weight -6 and -8, respectively. s takes values in $\{\pm 2, 0\}$, while t takes values in $\{\pm 4, \pm 2, 0\}$.

The intersection matrix Q associated to the plumbing is:

$$Q = \begin{pmatrix} -2 & 1 & 1 & 1 & 0 & 0 & 0 & 0 & 0 \\ 1 & -2 & 0 & 0 & 0 & 0 & 0 & 0 & 0 \\ 1 & 0 & -6 & 0 & 0 & 0 & 0 & 0 & 0 \\ 1 & 0 & 0 & -2 & 1 & 0 & 0 & 0 & 0 \\ 0 & 0 & 0 & 1 & -2 & 1 & 0 & 0 & 0 \\ 0 & 0 & 0 & 0 & 1 & -2 & 1 & 0 & 0 \\ 0 & 0 & 0 & 0 & 0 & 1 & -2 & 1 & 0 \\ 0 & 0 & 0 & 0 & 0 & 0 & 1 & -2 & 1 \\ 0 & 0 & 0 & 0 & 0 & 0 & 0 & 1 & -8 \end{pmatrix},$$

and its inverse is

$$Q^{-1} = -\frac{1}{256} \begin{pmatrix} 516 & 258 & 86 & 432 & 348 & 264 & 180 & 96 & 12 \\ 258 & 257 & 43 & 216 & 174 & 132 & 90 & 48 & 6 \\ 86 & 43 & 57 & 72 & 58 & 44 & 30 & 16 & 2 \\ 432 & 216 & 72 & 576 & 464 & 352 & 240 & 128 & 16 \\ 348 & 174 & 58 & 464 & 580 & 440 & 300 & 160 & 20 \\ 264 & 132 & 44 & 352 & 440 & 528 & 360 & 192 & 24 \\ 180 & 90 & 30 & 240 & 300 & 360 & 420 & 224 & 28 \\ 96 & 48 & 16 & 128 & 160 & 192 & 224 & 256 & 32 \\ 12 & 6 & 2 & 16 & 20 & 24 & 28 & 32 & 36 \end{pmatrix}.$$

Therefore, in the same notation as in the proof of Proposition 3.1,

$$\frac{c_1^2(J_{s,t}) - 2\chi(P^*) - 3\sigma(P^*)}{4} = \frac{2304 - 57s^2 - 4st - 36t^2}{256},$$

and the minimum of this function as s and t vary in the corresponding ranges is 0, attained only at $(s,t) = \pm(4,6)$; that is, only at the canonical contact structure and its conjugate. □

4. Background on symplectic configuration of curves

We will briefly collect some background related to rational cuspidal curves and embedding classifications that we will use repeatedly in the remaining sections of the paper. For further details, see [GS22, Sections 2 and 3] (see also [Lis08]).

By [Wal04], every complex plane curve singularity can be resolved by blowing up (sufficiently many times), and the diffeomorphism type of the link determines the topology of the resolution. There are two natural stopping points when resolving a singularity: the *minimal resolution* is the smallest resolution such that the proper transform $\widetilde{C}$ of C is smooth; the *normal crossing resolution* is the smallest resolution such that the total transform $\overline{C}$ of C is a normal crossing divisor, i.e. all singularities are double points.

The *multiplicity* m_p of a singular point p of a curve C is the minimal intersection of a germ of a divisor D at p with C. In terms of the resolution, m_p is the algebraic intersection number of the exceptional divisor and the proper transform after blowing up at p, and we have $[\widetilde{C}] = [C] - m_p[E]$. The *multiplicity sequence* of a singularity p is defined as the sequence of multiplicities of the curve at p and each of its proper transforms in the sequence of blow-ups leading to the minimal resolution of the singularity.

Recall that an isolated singularity of a curve at q can be smoothed to its Milnor fiber. Let $\mu(q)$ denote the first Betti number of the Milnor fiber. If q has r local branches, define $\delta(q)$ by $2\delta(q) = \mu(q) + r - 1$. If q is a cusp, then $\delta(q)$ is the genus of its Milnor fiber. It follows from the adjunction formula that for a singularity with multiplicity sequence $[m_1, \dots, m_n]$

$$\delta(p) = \frac{1}{2} \sum m_j(m_j - 1). \tag{4.1}$$

There are two different types of notions of the genus of a singular curve C: the *geometric genus* and the *arithmetic genus*. The geometric genus $p_g(C)$ is the genus of the proper transform of the curve in the minimal resolution; by definition, rational curves have geometric genus zero. The arithmetic genus $p_a(C)$ is given by

$$p_a(C) := p_g(C) + \sum_{p \in \mathrm{Sing}(C)} \delta(p) \tag{4.2}$$

Next, we will state various results about embedded surfaces in symplectic 4-manifolds that we used heavily in our embedding classification results in [GS22], beginning with the following important result of McDuff.

Theorem 4.1 ([McD90]). *If (X, ω) is a closed symplectic 4-manifold and $C_0 \subset X$ is a smooth symplectic sphere of self-intersection number $+1$, then there is a symplectomorphism of (X, ω) to a symplectic blow up of $(\mathbb{CP}^2, \lambda\omega_{\mathrm{FS}})$ for some $\lambda > 0$, such that C_0 is identified with $\mathbb{CP}^1$.*

This theorem motivates our focus on surfaces embedded in $\mathbb{CP}^2\#N\overline{\mathbb{CP}}^2$. We will use the standard basis $h, e_1, \dots, e_N$ for $H_2(\mathbb{CP}^2\#N\overline{\mathbb{CP}}^2)$ with $h^2 = 1$ and $e_i^2 = -1$. The following is a useful lemma to find embedded exceptional spheres which intersect a given collection of symplectic surfaces positively.

Lemma 4.2 ([McD90], [GS22, Lemma 3.5]). *Suppose $\mathcal{C}$ is a configuration of positively intersecting symplectic surfaces in $\mathbb{CP}^2\#N\overline{\mathbb{CP}}^2$. Let $e_{i_1}, \dots, e_{i_\ell}$ be exceptional classes which have non-negative algebraic intersections with each of the symplectic surfaces in the configuration $\mathcal{C}$. Then there exist disjoint exceptional spheres $E_{i_1}, \dots, E_{i_\ell}$ representing the classes $e_{i_1}, \dots, e_{i_\ell}$ respectively such that any geometric intersections of E with $\mathcal{C}$ are positive.*

Using the previous lemma, information about an embedding of surfaces in $\mathbb{CP}^2\#N\overline{\mathbb{CP}}^2$ can be reduced to symplectic isotopy classes of curve configurations in $\mathbb{CP}^2$ together with the information of the homology classes represented by the surface components. Using the adjunction formula, we have the following restrictions on the homology classes that can represent a symplectic sphere in $\mathbb{CP}^2\#N\overline{\mathbb{CP}}^2$.

Lemma 4.3 ([GS22, Lemma 3.7]). *Suppose Σ is a smooth symplectic sphere in $\mathbb{CP}^2\#N\overline{\mathbb{CP}}^2$ intersecting $\mathbb{CP}^1$ non-negatively. Then writing $[\Sigma] = ah + a_0e_0 + \cdots + a_{N-1}e_{N-1}$ (so $a \geq 0$), we have:*

1) *$\sum(a_i^2 + a_i) = 2 + a^2 - 3a$.*
2) *If $a = 0$, there is one i_0 such that $a_{i_0} = 1$ and all other $a_i \in \{0, -1\}$.*
3) *If $a \neq 0$, then for all i, $a_i \leq 0$.*

Some particular cases which we will use often are:

4) *If $a = 1$ or $a = 2$, $a_i \in \{0, -1\}$ for all i.*
5) *If $a = 3$, then there exists a unique i_0 such that $a_{i_0} = -2$, and $a_i \in \{0, -1\}$ for all other i.*

The self-intersection number of Σ can be used to compute how many a_i have coefficient 0 versus -1.

In the following lemmas from [GS22], C_i and C_j are smooth symplectic spheres in $\mathbb{CP}^2\#N\overline{\mathbb{CP}}^2$ such that $[C_i]\cdot h = [C_j]\cdot h = 0$ and $[C_i]\cdot[C_j] \geq 0$ whenever $i \neq j$. These are easy consequences of Lemma 4.3 and the hypothesized intersection relations.

Lemma 4.4 ([GS22, Lemmas 3.8 and 3.10]). *If $[C_i]\cdot[C_j] = 1$ (and $[C_i]\cdot h = [C_j]\cdot h = 0$), there is exactly one exceptional class e_i which appears with non-zero coefficient in both $[C_i]$ and $[C_j]$. The coefficient of e_i is $+1$ in one of $[C_i], [C_j]$ and -1 in the other.*

If $[C_i]\cdot[C_j] = 0$, then either there is no exceptional class which appears with non-zero coefficients in both, or there are exactly two exceptional classes e_m and e_n appearing with non-zero coefficients in both. One of these classes e_m has coefficient -1 in both $[C_i]$ and $[C_j]$ and the other e_n appears with coefficient $+1$ in one of $[C_i]$ or $[C_j]$ and coefficient -1 in the other.

Lemma 4.5 ([GS22, Lemma 3.9]). *If e_m appears with coefficient $+1$ in $[C_i]$ then it does not appear with coefficient $+1$ in $[C_j]$.*

Lemma 4.6 ([GS22, Lemmas 3.11 and 3.12]). *Suppose $C_1, \ldots, C_k$ are a linear chain of symplectic spheres of self-intersection -2 disjoint from $\mathbb{CP}^1$ in $\mathbb{CP}^2\#N\overline{\mathbb{CP}}^2$ ($[C_i]\cdot[C_j] = 1$ $|i-j| = 1$ and 0 otherwise). Then the homology classes are given by one of the following two options up to reindexing the exceptional classes:*

(A) $[C_i] = e_i - e_{i+1}$ *for* $i = 1, \ldots, k$.

(B) $[C_i] = e_{i+1} - e_i$ *for* $i = 1, \ldots, k$.

In the homology class of any surface disjoint from the chain, the coefficients for $e_1, \ldots, e_{k+1}$ are equal.

If the chain is attached to another symplectic sphere C_0 which does intersect $\mathbb{CP}^1$, option (B) can only occur if $e_2, \ldots, e_{k+1}$ all appear with coefficient -1 in $[C_0]$. In particular if $[C_0]\cdot h = 1$, option (B) can only occur if $[C_0]^2 \leq 1 - k$.

5. Rational blow-down relations for fillings of unicuspidal contact manifolds

Next we study the relationships between different fillings of contact manifolds (Y_C, ξ_C), where C is a symplectic curve in $\mathbb{CP}^2$ with a single $T(a,b)$ cusp. The relationship we will focus on is symplectic *rational blow-down* (in its most general sense) which means replacing a plumbing of symplectic

spheres with a symplectic rational homology ball filling. The first examples of rational blow-down were introduced by Fintushel and Stern [FS97], shown to be symplectic operations by Symington [Sym98] and were generalized in [Par97, Sym01, SSW08]. In [BS11], Bhupal and Stipsicz show that these examples are all the plumbings which can be symplectically rationally blown down, and explicitly list out all families of non-linear plumbings which admit symplectic rational blow-downs.

Linear plumbings which can be symplectically rationally blown down have boundaries which are the lens spaces $L(p^2, pq-1)$. The associated plumbing graphs for this family all arise recursively as an iterated "2-expansion" of (-4), where a 2-expansion of a linear plumbing with weights $(-a_1, \dots, -a_{n-1})$ can be either $(-a_1-1, \dots, -a_{n-1}, -2)$ or $(-2, -a_1, \dots, -a_{n-1}-1)$. This can be understood as starting with a -4-sphere and a -1-sphere intersecting at two points transversally, and iteratively blowing up at one of the two intersection points on a -1-sphere, and then looking at the linear plumbing that results from removing the -1-sphere after all of the blow-ups. Observe that "interior" vertices cannot be changed by 2-expansions. In particular, an interior vertex of square strictly less than -2 survives after 2-expansions.

Now we proceed to study when different fillings of (Y_C, ξ_C) are related by sequences of symplectic rational blow-downs. Note that among the curves in $\mathbb{CP}^2$ with a single $T(a,b)$ cusp, the two exceptional cases are the only cases where the symplectic rational blow-down relations have not already been established in prior work. In the $\mathcal{A}_p$ family, there is a unique minimal symplectic filling so there are no pairs to relate. In the $\mathcal{B}_p$ case, there are two fillings which are related by a single rational blow-down of a -4-sphere [GS22, Proposition 6.6]. The Fibonacci families have Y_C a lens space or connected sum of lens spaces. Symplectic rational blow-down relations between lens spaces were established in [BO16]. The minimal symplectic fillings of the connected sum of two lens spaces are all Stein because the contact manifolds are planar [Wen10]. Thus they are boundary sums of Stein fillings of the two lens space summands [Eli90], so the results of [BO16] apply in this case as well.

We begin with the first exceptional case where C has a cusp of type $T(3,22)$ and self-intersection number 64. The minimal symplectic fillings of (Y_C, ξ_C) are each obtained as the complement of a concave neighborhood of an embedding of C (or any of its resolutions) into a closed symplectic 4-manifold. In [GS22] we classified all relatively minimal symplectic embeddings of the minimal resolution of C. The minimal resolution of C in this case

is described by the graph below where the triple edge indicates a tangency of multiplicity three between the $+1$-sphere and the -1-sphere.

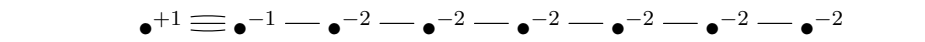

In [GS22, Section 6], we prove that there are exactly three symplectic isotopy classes of relatively minimal embeddings of this minimal resolution into closed symplectic manifolds. The three isotopy classes are distinguished by the maps induced by the embeddings on second homology which are given by the three possibilities below. Note that in each case the embedding is into a blow-up of $\mathbb{CP}^2$ and we use the standard generators $h, e_0, \ldots, e_{N-1} \in H_2(\mathbb{CP}^2 \# N\overline{\mathbb{CP}}^2; \mathbb{Z})$ represented by $\mathbb{CP}^1 \subset \mathbb{CP}^2$ and the exceptional spheres. The vertices in the graph above correspond to generators of the second homology of the concave neighborhood of the minimal resolution, and the three possibilities for their images in $H_2(\mathbb{CP}^2 \# N\overline{\mathbb{CP}}^2; \mathbb{Z})$ under different symplectic embeddings are (with $N = 13, 8, 7$ respectively):

$$h, 3h - 2e_0 - e_1 - e_2 - e_3 - e_4 - e_5 - e_6, e_1 - e_7, e_7 - e_8, e_8 - e_9, e_9 - e_{10}, e_{10} - e_{11}, e_{11} - e_{12},$$
$$h, 3h - 2e_0 - e_1 - e_2 - e_3 - e_4 - e_5 - e_6, e_1 - e_7, e_2 - e_1, e_3 - e_2, e_4 - e_3, e_5 - e_4, e_6 - e_5,$$
$$h, 3h - 2e_0 - e_1 - e_2 - e_3 - e_4 - e_5 - e_6, e_0 - e_1, e_1 - e_2, e_2 - e_3, e_3 - e_4, e_4 - e_5, e_5 - e_6.$$

The fillings of (Y_C, ξ_C) are the complements of these embeddings, which have $b_2 = N - 7$. Therefore we have three fillings, V_6, V_1, and V_0, where the indices are chosen so that $b_2(V_k) = k$. As a corollary to Proposition 3.1, V_6 is symplectic deformation equivalent to the negative definite symplectic plumbing (3.1).

Proposition 5.1. *There is a linear symplectic rational blow-down from V_6 to V_1 and a non-linear symplectic rational blow-down from V_6 to V_0, but no rational blow-down from V_1 to V_0.*

Note that any sequence of symplectic rational blow-downs will yield a sequence of symplectic fillings. Since we have a classification of the fillings of (Y_C, ξ_C), it suffices to understand when any pair of these symplectic fillings is related by a single symplectic rational blow-down.

Proof of Proposition 5.1. It is apparent from the plumbing description of V_6, that there is a linear plumbing of symplectic spheres with self-intersections $(-8, -2, -2, -2, -2)$. This is one of Fintushel–Stern's original rational blow-downs $L(p^2, p-1)$ with $p = 6$. Rationally blowing down this chain yields a symplectic filling with $b_2 = 1$, so it is necessarily V_1.

Since V_6 itself is a plumbing, its replacement by the rational homology ball filling V_0 is itself a rational blow-down relation, and indeed this plumbing coincides with the plumbing of Figure 1(f) with $q = 2$ in [BS11].

We now show that there is no rational blow-down from V_1 to V_0. There is a unique plumbing with $b_2 = 1$ which can be rationally blown down which is a -4-sphere. The non-torsion part of $H_2(V_1)$ is generated by the orthogonal complement of the classes in the corresponding embedding, namely $3e_0 - e_1 - \cdots - e_7$. Therefore the intersection form of V_1 is $\langle -16 \rangle$, so no homology class has self-intersection -4. Thus there can be no rational blow-down from V_1 to V_0. □

Next we consider the second exceptional case, where C has a singularity of type $(6, 43)$ and self-intersection number 16^2. Again, the minimal symplectic fillings of (Y_C, ξ_C) are precisely the complements of the relatively minimal symplectic embeddings of a given resolution of C into closed symplectic manifolds. We will consider a resolution which is between the minimal and minimal normal crossing resolution indicated by the graph below. Here the $+1$- and -4-spheres intersect tangentially with multiplicity 3, and the -1-sphere intersects these two at the same point transversally.

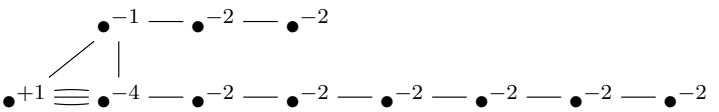

Again, we have results from [GS22, Section 6] classifying the symplectic isotopy classes of relatively minimal embeddings of this resolution. In this case, there are six such embeddings distinguished by the maps they induce on second homology which are given as follows.

Let W_9 denote the filling complementary to the embedding of the resolution into $\mathbb{CP}^2 \# 18\overline{\mathbb{CP}}^2$ with homology classes:

$$\begin{array}{cccccccc} & h - e_0 - e_{16}, & & e_{16} - e_{17}, & e_{17} - e_{18} & & & \\ h, & 3h - 2e_0 - e_1 - \cdots - e_9, & e_1 - e_{10}, & e_{10} - e_{11}, & e_{11} - e_{12}, & e_{12} - e_{13}, & e_{13} - e_{14}, & e_{14} - e_{15} \end{array}$$

Let W_6 denote the filling complementary to the embedding of the resolution into $\mathbb{CP}^2 \# 16\overline{\mathbb{CP}}^2$ with homology classes:

$$\begin{array}{cccccccc} & h - e_8 - e_9, & & e_8 - e_7, & e_9 - e_8 & & & \\ h, & 3h - 2e_0 - e_1 - \cdots - e_9, & e_1 - e_{10}, & e_{10} - e_{11}, & e_{11} - e_{12}, & e_{12} - e_{13}, & e_{13} - e_{14}, & e_{14} - e_{15} \end{array}$$

Let Z_6 denote the filling complementary to the embedding of the resolution into $\mathbb{CP}^2\#16\overline{\mathbb{CP}}^2$ with homology classes:

$$\begin{array}{lllllllll} & h-e_8-e_9, & & e_8-e_7, & e_7-e_6 & & & & \\ h, & 3h-2e_0-e_1-\cdots-e_9, & e_1-e_{10}, & e_{10}-e_{11}, & e_{11}-e_{12}, & e_{12}-e_{13}, & e_{13}-e_{14}, & e_{14}-e_{15} \end{array}$$

Let W_4 denote the filling complementary to the embedding of the resolution into $\mathbb{CP}^2\#14\overline{\mathbb{CP}}^2$ with homology classes:

$$\begin{array}{lllllllll} & h-e_0-e_{11}, & & e_{11}-e_{12}, & e_{12}-e_{13} & & & & \\ h, & 3h-2e_0-e_1-\cdots-e_9, & e_1-e_{10}, & e_2-e_1, & e_3-e_2, & e_4-e_3, & e_5-e_4, & e_6-e_5 \end{array}$$

Let W_1 denote the filling complementary to the embedding of the resolution into $\mathbb{CP}^2\#11\overline{\mathbb{CP}}^2$ with homology classes:

$$\begin{array}{lllllllll} & h-e_8-e_9, & & e_8-e_7, & e_9-e_8 & & & & \\ h, & 3h-2e_0-e_1-\cdots-e_9, & e_1-e_{10}, & e_2-e_1, & e_3-e_2, & e_4-e_3, & e_5-e_4, & e_6-e_5 \end{array}$$

Let W_0 denote the filling complementary to the embedding of the resolution into $\mathbb{CP}^2\#10\overline{\mathbb{CP}}^2$ with homology classes:

$$\begin{array}{lllllllll} & h-e_8-e_9 & & e_8-e_7 & e_9-e_8 & & & & \\ h, & 3h-2e_0-e_1-\cdots-e_9, & e_0-e_1, & e_1-e_2, & e_2-e_3, & e_3-e_4, & e_4-e_5, & e_5-e_6 \end{array}$$

Observe that the subscript indicates the second Betti number. A posteriori, due to Proposition 3.3, W_9 is the plumbing of symplectic spheres according to the graph in (3.2).

Proposition 5.2. *Let C be the rational cuspidal curve with a single $T(6,43)$ singularity and self-intersection number 16^2. There exists a rational blow-down of a connected embedded plumbing of symplectic spheres from one filling of (Y_C,ξ_C) to another if and only if there is an edge between the fillings in following graph.*

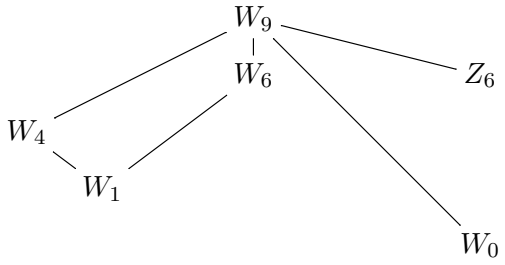

Proof. First, we observe the existence of the rational blow-downs from W_9 to W_6 and W_4, and from W_6 and W_4 to W_1. Using the fact that W_9 is

necessarily the plumbing (3.2) (by Proposition 3.3), we can visibly see sub-plumbings of the form $(-8,-2,-2,-2,-2)$ and $(-6,-2,-2)$. Note that these symplectic embeddings are not unique, but it is possible to realize disjoint embeddings of both the $(-8,-2,-2,-2,-2)$ and $(-6,-2,-2)$ chains as disjoint sub-plumbings. Rationally blowing down a $(-8,-2,-2,-2,-2)$ chain yields a symplectic filling with $b_2 = 4$ which is necessarily W_4. Rationally blowing down a $(-6,-2,-2)$ chain yields symplectic fillings with $b_2 = 6$, which must be either W_6 or Z_6. Rationally blowing down disjoint plumbings $(-8,-2,-2,-2,-2)$ and $(-6,-2,-2)$ yields a symplectic filling with $b_2 = 1$, so it must be W_1. Using the homological properties that define Z_6, we will show below that Z_6 does not admit any further rational blow-downs. Therefore, rationally blowing down a $(-6,-2,-2)$ plumbing in W_9 which is disjoint from a $(-8,-2,-2,-2,-2)$ plumbing, necessarily results in W_6. This shows as well that there is a further rational blow-down from W_6 to W_1. If we exchange the order of which of the two disjoint plumbings we rationally blow-down first, we see the sequence of rational blow-downs from W_9 to W_4 to W_1.

Next, we will show there is a rational blow-down from W_9 to Z_6. Consider the $(-6,-2,-2)$ chain embedded as a sub-plumbing of W_9 given by turning right instead of left at the 3-valent vertex. This sub-plumbing is not disjoint from the $(-8,-2,-2,-2,-2)$ chain, and thus potentially yields a different result from the rational blow-down of the other embedding of the $(-6,-2,-2)$ chain (where you turn left at the 3-valent vertex). We will now verify that rationally blowing down this embedding of the $(-6,-2,-2)$ plumbing is not W_6, and thus must be Z_6.

First, we argue that the result of this rational blow-down is simply connected. Since W_9 is a tree plumbing of spheres, it is simply connected. The fundamental group of the rational homology ball which replaces the $(-6,-2,-2)$ plumbing is normally generated by the meridian of the last -2-sphere in the chain, so it suffices to show this curve is null-homotopic in the complement of the plumbing in W_9. This meridian can be realized as the equator of the next -2-sphere S in the W_9 plumbing, so it bounds a disk (the other half of the -2-sphere S) in the complement of the $(-6,-2,-2)$ chain. Consequently the result of this rational blow-down is a simply-connected filling, and in particular it has trivial H_1.

We will next show that W_6 necessarily has non-trivial H_1. To see this, consider the long exact sequence of the pair $(W_6, \partial W_6)$:

$$0 = H_2(\partial W_6) \to H_2(W_6) \to H_2(W_6, \partial W_6) \cong H^2(W_6) \to H_1(\partial W_6) \cong \mathbb{Z}/256\mathbb{Z}$$

Here we identify $H_2(W_6, \partial W_6) \to H^2(W_6)$ by Alexander–Lefschetz duality. Under this identification, the map $H_2(W_6) \to H^2(W_6)$ in the sequence is described by the intersection form Q_{W_6} of W_6, by sending $a \in H_2(W_6)$ to $Q_{W_6}(a, \cdot)$. The size of the cokernel of this map is the determinant of Q_{W_6}. In [GS22, Proof of Theorem 6.6, pp. 1652–1653], we computed the intersection forms for W_6 and Z_6, by finding an integral homology basis for the orthogonal complement in $H_2(\mathbb{CP}^2 \# 16\overline{\mathbb{CP}}^2)$ of the corresponding embeddings of the resolutions for W_6 and Z_6 (which are listed above). We calculated that $\det(Q_{W_6}) = 64$ and $\det(Q_{Z_6}) = 256$. (Note, this distinguishes W_6 from Z_6.) On the other hand, $H_1(\partial W_6) \cong \mathbb{Z}/256\mathbb{Z}$ since $\partial W_6 = -S^3_{256}(T(6, 43))$. Since the co-kernel of the map $H_2(W_6) \to H^2(W_6)$ has order 64, the map from $H^2(W_6)$ to $H_1(\partial W_6) \cong \mathbb{Z}/256\mathbb{Z}$ cannot be surjective. Therefore, there are some elements which are not in the kernel of the map $H_1(\partial W_6) \to H_1(W_6)$, so $H_1(W_6) \neq 0$. This shows that the rational blow-down of this embedding of the $(-6, -2, -2)$ chain is necessarily Z_6.

Finally, the entirety of the W_9 plumbing can be rationally blown down in a non-linear way (this plumbing is [BS11, Figure 1(j)] for $q = 4$) to W_0.

Next, we will show that fillings which are not connected by edges are not related by a symplectic rational blow-down. Note that because rational blow-down strictly decreases b_2, we only need to obstruct rational blow-downs from larger fillings to smaller fillings.

We will next show that Z_6 cannot be symplectically rationally blown down to any other filling. To do this, we start by looking at the classes in $H_2(Z_6)$ which could be represented by a symplectic sphere. Classes in $H_2(Z_6)$ must be in the orthogonal complement of the classes listed above for the Z_6 embedding of the resolution in $H_2(\mathbb{CP}^2 \# 16\overline{\mathbb{CP}}^2)$. Classes in this orthogonal complement are classes of the form $\sum_{i=0}^{15} a_i e_i$ where

$$a_1 = a_{10} = \cdots = a_{15}, \qquad a_6 = a_7 = a_8 = -a_9, \qquad 2a_0 + a_1 + \cdots + a_9 = 0$$

where, using the equalities above, the last equation can equivalently be written as

$$2a_0 + a_1 + \cdots + a_5 + 2a_6 = 0. \tag{5.1}$$

If the class represents a symplectic sphere, by Lemma 4.3, there exists an index $i_0 \in \{0, \ldots, 15\}$ such that $a_{i_0} = 1$ and $a_i \in \{-1, 0\}$ for all $i \neq i_0$. Combining this with the forced equalities of coefficients above, we see that $i_0 \notin \{1, 6, 7, 8, 10, \ldots, 15\}$. Furthermore $i_0 \neq 9$ because if $a_9 = 1$, $a_6 = a_7 = a_8 = -1$, but then there are no solutions to Equation (5.1) if $a_0, \ldots, a_5 \in \{0, -1\}$.

Therefore the only possibilities are that $i_0 \in \{0, 2, 3, 4, 5\}$, and we get the following possibilities:

$$\begin{aligned}
&e_0 - e_1 - e_{10} - \cdots - e_{15} - e_i, && 2 \leq i \leq 5\\
&e_0 - e_i - e_j, && 2 \leq i < j \leq 5\\
&e_i - e_1 - e_{10} - \cdots - e_{15}, && 2 \leq i \leq 5\\
&e_i - e_j, && 2 \leq i \neq j \leq 5.
\end{aligned}$$

Note that classes of the first type have square -9, the second type have square -3 and the third type have square -8, and the last have square -2. In particular, any symplectic plumbing of spheres which embeds in Z_6 can only include spheres with self-intersection numbers in the set $\{-2, -3, -8, -9\}$.

We start with a general observation: any plumbing of spheres which can be symplectically rationally blown down contains at least one sphere with self-intersection strictly less than -3. For linear plumbings this follows from the fact that they are all obtained as 2-expansions of (-4), and for non-linear plumbings this follows from inspection of the families in [BS11] (note the parameters p, q, r must be non-negative).

Therefore, the only possible plumbings that may be symplectically rationally blown down which can embed in Z_6 must include at least one sphere of self-intersection -8 or -9. Because $b_2(Z_6) = 6$, any embeddable plumbing must have $b_2 \leq 6$. The only 2-expansion of (-4) of length ≤ 6 which includes a -9-sphere is $(-9, -2, -2, -2, -2, -2)$. Those that include a -8-sphere are $(-2, -8, -2, -2, -2, -3)$ and $(-8, -2, -2, -2, -2)$. For the non-linear plumbings in [BS11], we can immediately rule out embeddings of plumbings in Figure 1(a),(e),(h),(i),(j) and 2(a),(b),(c) because they contain either -4- or -6-spheres. We rule out 1(b),(c),(d),(g) because any plumbing in these families has $b_2 > 6$ when self-intersections are restricted to lie in $\{-2, -3, -8, -9\}$. Thus the only non-linear plumbing which could be rationally blown down with $b_2 \leq 6$, and self-intersection numbers in this class is the case of [BS11, Figure 1(f) with $q = 2$], which happens to be the plumbing (3.1). We will rule out these remaining cases now using the pairwise intersections of these classes (we will freely use the lemmas of Section 4). If there were an embedding of the linear plumbing $(-9, -2, -2, -2, -2, -2)$ in Z_6, up to permuting the indices $\{2, 3, 4, 5\}$, the first sphere in the chain would represent $e_0 - e_1 - e_{10} - \cdots - e_{15} - e_2$, and the next three must represent $e_2 - e_3$, $e_3 - e_4$, $e_4 - e_5$ (in order for these spheres to have pairwise intersections according to the linear chain). This leaves no possibility $e_i - e_j$, $i, j \in \{2, 3, 4, 5\}$ for the fourth -2-sphere in the chain which has intersection 0 with the first two -2-spheres and 1 with the third. An embedding of

$(-8,-2,-2,-2,-2)$ would necessarily (up to a permutation of $\{2,3,4,5\}$) have the first four spheres in homology classes $e_2 - e_1 - e_{10} - \cdots - e_{15}$, $e_3 - e_2$, $e_4 - e_3$, $e_5 - e_4$, leaving no possible $i, j \in \{2,3,4,5\}$ such that $e_i - e_j$ could have intersection $+1$ with $e_5 - e_4$ and intersection 0 with the first three classes. Note that the non-linear plumbing (3.1) which is case 1(f) on the Bhupal–Stipsicz list, contains the linear chain $(-8,-2,-2,-2,-2)$ as a sub-plumbing so this non-linear plumbing is also obstructed from symplectically embedding into Z_6. Similarly, an embedding of the linear chain $(-2,-8,-2,-2,-2,-3)$ would (up to permutation of $\{2,3,4,5\}$) have the first four spheres in classes, $e_2 - e_3$, $e_3 - e_1 - e_{10} - \cdots - e_{15}$, $e_4 - e_3$, $e_5 - e_4$, leaving no options for the fifth sphere in the chain with the correct intersection number. Thus there is no embedding into Z_6 of any plumbing which can be symplectically rationally blown down.

Note at this point, we have established that Z_6 cannot be the filling which results from rationally blowing down the $(-6,-2,-2)$ chain in W_9 which is disjoint from the $(-8,-2,-2,-2,-2)$ chain (since Z_6 admits no further rational blow-downs). Because W_6 is the only other symplectic filling with $b_2 = 6$, W_6 is necessarily the result of the rational blow-down of this disjoint $(-6,-2,-2)$ chain in W_9. This establishes that W_6 can be rationally blown down to W_1, and gives another way to see that W_6 and Z_6 are not symplectomorphic.

Next, we will similarly obstruct rational blow-downs from W_6 to W_4 and W_0, though the obstruction to a rational blow-down to W_0 will be significantly more subtle. In this case, the orthogonality relations imply classes in $H_2(W_6;\mathbb{Z})$ are precisely those of the form $\sum_{i=0}^{15} a_i e_i$ where

$$a_7 = a_8 = a_9 = 0, \qquad a_1 = a_{10} = \cdots = a_{15}, \qquad 2a_0 + a_1 + \cdots + a_6 = 0.$$

Proceeding as before, the classes satisfying these constraints which are represented by symplectic spheres are

$$\begin{array}{ll} e_0 - e_1 - e_{10} + \cdots - e_{15} - e_i, & 2 \le i \le 6 \\ e_0 - e_i - e_j, & 2 \le i < j \le 6 \\ e_i - e_1 - e_{10} + \cdots - e_{15}, & 2 \le i \le 6 \\ e_i - e_j, & 2 \le i \ne j \le 6. \end{array}$$

Note that the squares of these classes are $\{-9,-3,-8,-2\}$. Since the only plumbing with $b_2 = 2$ which can be rationally blown down is $(-5,-2)$ and there are no symplectic -5-spheres in W_6, there can be no symplectic rational blow-down from W_6 to W_4. We can obstruct the embeddings into W_6 of symplectic linear plumbings of with $b_2 = 6$ as before. The only

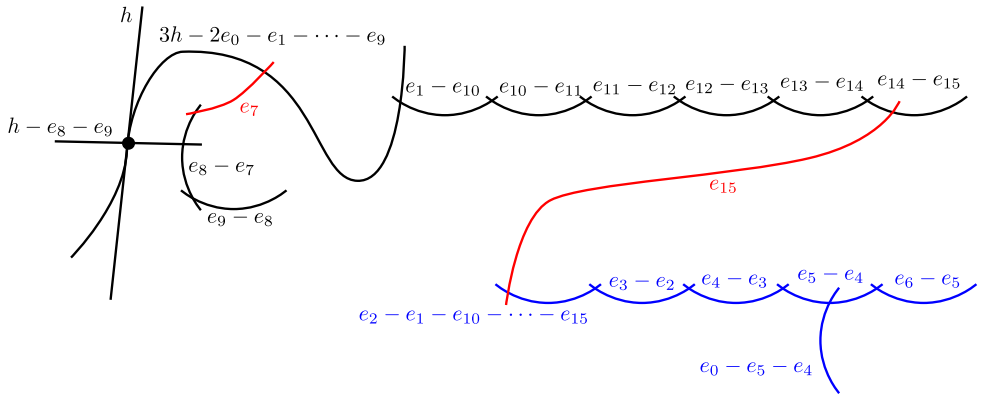

Figure 12. Embedding into $\mathbb{CP}^2\#16\overline{\mathbb{CP}}^2$ of the resolution complementary to W_6, together with a hypothesized disjoint plumbing with the homology classes of each component specified, as well as exceptional spheres representing e_7 and e_{15}.

two possibilities are $(-9,-2,-2,-2,-2,-2)$ and $(-2,-8,-2,-2,-2,-3)$. In the former case, the first five spheres in the chain would necessarily (up to permuting indices $\{2,\dots,6\}$) represent $e_0 - e_1 - e_{10} - \cdots - e_{15} - e_2$, $e_2 - e_3$, $e_3 - e_4$, $e_4 - e_5$, $e_5 - e_6$, leaving no option for the sixth sphere in the chain. In the latter case, the chain would need to take the form $e_3 - e_2$, $e_2 - e_1 - e_{10} - \cdots - e_{15}$, $e_4 - e_2$, $e_5 - e_4$, $e_6 - e_5$, $e_0 - e_6 - e_j$ for some $j \in \{2,\dots,5\}$, but any value of j would result in a non-zero intersection of the last sphere in the chain with one of the first four spheres.

Next we consider potential non-linear plumbings which can be rationally blown down. In fact, there is a unique non-linear plumbing from the Bhupal–Stipsicz list with $b_2 = 6$ which we cannot rule out with homology classes alone. This is the plumbing [BS11, Figure 1(f)] for $q = 2$, which happens to be the plumbing (3.1) (the filling of the other exceptional cuspidal contact manifold). This consists of a linear chain $(-8,-2,-2,-2,-2)$ with an additional -3-sphere intersecting the second to last -2-sphere. Up to permutation of indices $\{2,\dots,6\}$, the spheres in the linear chain necessarily represent $e_2 - e_1 - e_{10} - \cdots - e_{15}$, $e_3 - e_2$, $e_4 - e_3$, $e_5 - e_4$, $e_6 - e_5$ and the additional -3-sphere would represent $e_0 - e_5 - e_6$. Since all of these classes could be represented by symplectic spheres in W_6, obstructing this rational blow-down is a little more subtle.

Suppose there exists such a symplectic plumbing in W_6. By gluing the concave neighborhood of the resolution, this is equivalent to assuming that

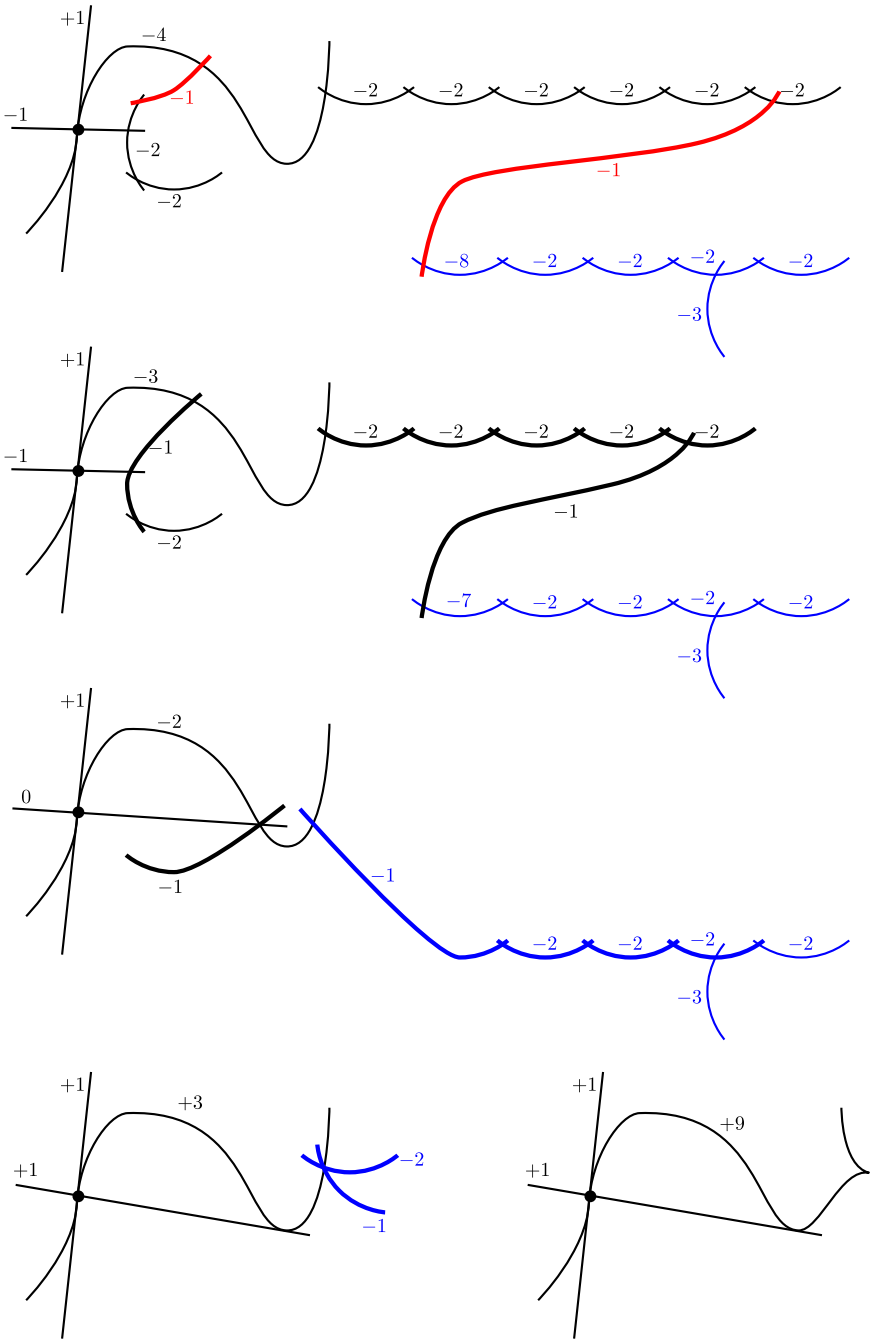

Figure 13. Sequence of blow-downs from $\mathbb{CP}^2\#16\overline{\mathbb{CP}}^2$ to $\mathbb{CP}^2$, starting with the configuration of Figure 12, and tracking the image under the blow-downs, ending with a cuspidal cubic and two lines (one tangent to order 3 and the other tangent to order 2 and passing through the inflection point). At each stage, the thickened curves indicate the curves which are blown down to get to the next figure in the sequence.

in $\mathbb{CP}^2\#16\overline{\mathbb{CP}}^2$, there exists an embedding of the resolution configuration (with homology classes as specified for W_6) and a disjoint embedding of the plumbing (3.1) representing homology classes as described above. Observe that the classes e_7 and e_{15} intersect all of the components in these two configurations non-negatively. Therefore, by Lemma 4.2, there exist embedded exceptional spheres representing e_7 and e_{15} which intersect all curve components in these configurations non-negatively (so the geometric and algebraic intersection numbers match). Consequently, we have an embedding into $\mathbb{CP}^2\#16\overline{\mathbb{CP}}^2$ of a configuration of curves as in Figure 12. Blowing down symplectic -1-spheres in this configuration representing e_i classes repeatedly as in Figure 13, we eventually reach a configuration of curves in $\mathbb{CP}^2$ consisting of the following components: a cubic C with a simple cusp at a point r, a line L which tangentially intersects C at an inflection point p (with multiplicity 3), and a line T which intersects C and L transversally at p, and intersects C tangentially (with multiplicity 2) at an additional point q. (Here r, p, q are all distinct points on C.) In fact, such a configuration of symplectic curves cannot exist, by the Riemann–Hurwitz formula. We fix an almost complex structure J such that C, L, and T are J-holomorphic. Then, using the pencil of J-holomorphic lines through p gives a degree-2 map $\pi\colon \mathbb{CP}^1 \to \mathbb{CP}^1$ with at least two ramification points (corresponding to the inflection line and the cusp respectively). Therefore Riemann–Hurwitz reads: $2 = 2 \cdot 2 - \sum(e_\pi(p) - 1)$, which implies that these are the only two ramification points, from which we deduce that there is no other tangent drawn to the cubic from the inflection point. (In fact, this exact argument appears in [GS22, p. 1652].) Thus, we reach a contradiction, and the plumbing (3.1) cannot embed symplectically in W_6, so we conclude there is no rational blow-down from W_6 to W_0.

To see there is no rational blow-down from W_4 to W_0, observe that $H_2(W_4)$ consists of classes $\sum_{i=0}^{13} a_i e_i$ where

$$\begin{aligned} &a_1 = a_2 = a_3 = a_4 = a_5 = a_6 = a_{10}, \\ &a_{11} = a_{12} = a_{13} = -a_0, \qquad 2a_0 + a_1 + \cdots + a_9 = 0. \end{aligned}$$

The classes of this form which can be represented by symplectic spheres are

$$\begin{aligned} &e_0 - e_i - e_j - e_{11} - e_{12} - e_{13}, \quad 7 \le i < j \le 9 \\ &e_i - e_j, \qquad\qquad\qquad\qquad\quad 7 \le i \ne j \le 9. \end{aligned}$$

These classes have squares -6 or -2. The only plumbing with $b_2 \le 4$ which can be symplectically rationally blown down and involves only -6- and -2-spheres is the linear chain $(-6, -2, -2)$ which connects W_4 to W_1. There is

no such plumbing of length 4 so there is no symplectic rational blow-down from W_4 to W_0.

The classes in $H_2(W_1)$ have the form $\sum_{i=0}^{10} a_i e_i$ such that

$$a_1 = a_2 = a_3 = a_4 = a_5 = a_6 = a_{10},$$
$$a_7 = a_8 = a_9 = 0, \qquad 2a_0 + a_1 + \cdots + a_9 = 0.$$

These are all integer multiples of $3e_0 - e_1 - \cdots - e_6 - e_{10}$ which has square -16, so there is no -4-sphere in W_1 to rationally blow down. □

Remark 5.3. Similar computations as seen in the previous proof which analyze the homology classes represented by symplectic spheres in V_6 proves that there is no linear rational blow-down from V_6 to V_0 in the case of $\mathcal{E}_3$, thus slightly strengthening the statement of Proposition 5.1. Similarly, one can obstruct the existence of a linear rational blow-down from W_9 to W_0. Such computations show that these non-linear rational blow-downs are genuinely new symplectic cut-and-paste operations, rather than just hidden reformulations of the prior known linear rational blow-downs.

6. Bounds on self-intersection numbers of rational cuspidal curves

In the earlier sections, we discussed symplectic fillings of contact manifolds (Y_C, ξ_C) arising on the concave boundary of a neighborhood of a rational cuspidal curve C whose algebraic genus and self-intersection number are determined by a degree which would allow the curve C to symplectically embed in $\mathbb{CP}^2$. In this section and the next, we study symplectic fillings for more general contact manifolds (Y_C, ξ_C) where self-intersection need not be d^2 and the arithmetic genus need not be a triangular number $\frac{1}{2}(d-1)(d-2)$.

C will be a singular symplectic curve with positive self-intersection number (and thus admitting a concave neighborhood). Recall that (Y_C, ξ_C) depends only on the singularity types, geometric genus, and self-intersection number of C. In this section, we will fix the singularity types for a rational (geometric genus equal to zero) curve, and vary the self-intersection number s. The goal is to prove that for certain values of s (depending on the singularities we fixed), (Y_C, ξ_C) is not symplectically fillable.

We begin with an easy, quite general remark.

Lemma 6.1. *Let C and C' be singular curves with the same geometric genus and configuration of singularities (not necessarily cuspidal), and* $0 <$

$C' \cdot C' \leq C \cdot C$. If (Y_C, ξ_C) is strongly symplectically fillable, then $(Y_{C'}, \xi_{C'})$ is strongly symplectically fillable as well.

Proof. Suppose (Y_C, ξ_C) has a strong symplectic filling W. Let N_C denote a standard concave neighborhood of C, and let (X, ω) denote the closed symplectic manifold which results from symplectically gluing N_C to W along their common contact boundary. Symplectically blow up X at $n := C \cdot C - C' \cdot C'$ smooth points of $C \subset X$. The proper transform of C yields a symplectic embedding of C' in $X \# n\overline{\mathbb{CP}}^2$. Since $C' \cdot C' > 0$, there exists a concave neighborhood of C' [GS22, Theorem 2.13] in $X \# n\overline{\mathbb{CP}}^2$ whose contact boundary is $(Y_{C'}, \xi_{C'})$. The complement of this neighborhood is a strong symplectic filling of $(Y_{C'}, \xi_{C'})$. □

Recall the definitions of the multiplicity sequence and $\delta(p)$ from Section 4, and that, for a cuspidal point p, $2\delta(p)$ is the sum of $m(m-1)$ over all elements m in the multiplicity sequence for p. Let $M(p)$ be the sum of the squares of all terms in the multiplicity sequence of the singularity at p. Let $\ell(p)$ denote the last (and smallest) entry in the multiplicity sequence. (Note that in our convention, $\ell(p) > 1$ because we define the multiplicity sequence using the minimal resolution rather than the normal crossing resolution.) Note that $M(p)$ (respectively, $M(p) + \ell(p)$) is the amount by which the self-intersection decreases when taking the minimal smooth (resp. normal crossing) resolution of p. For instance, when the singularity at p is of type $T_{m,km+1}$, the multiplicity sequence is $[m^{[k]}]$, so that $M(p) = km^2$, $\ell(p) = m$, and $\delta(p) = \frac{1}{2}km(m-1)$.

Proposition 6.2. *Suppose that C is a rational curve with cusp singularities $p_1, \ldots, p_\mu$ ($\mu \geq 1$), and with reducible singularities $q_1, \ldots, q_\nu$ ($\nu \geq 0$), and satisfying*

$$C \cdot C \geq \sum M(p_i) + \sum M(q_j) + 2 \min \ell(p_i) + 2.$$

Then (Y_C, ξ_C) is not strongly symplectically fillable. If additionally $p_1, \ldots, p_\mu$ are the only singularities of C (i.e. C is cuspidal), then ξ_C is not even weakly symplectically fillable.

Proof. Without loss of generality, suppose that p_1 is a singular cusp with $\ell(p_1) = \ell = \min \ell(p_i)$. By Lemma 6.1 above, it suffices to prove the statement for $C \cdot C = \sum M(p_i) + \sum M(q_i) + 2\ell + 2$.

Let (W, ω_W) be a strong symplectic filling of (Y_C, ξ_C), and (X', ω') be the closed symplectic manifold obtained by gluing a standard concave neighborhood of C to (W, ω_W). We now view C as a symplectic curve in X'.

Blow up C at all its singular points until we obtain the minimal smooth resolution of C, i.e. the proper transform $\widetilde{C}$ of C is a smooth sphere of self-intersection $\widetilde{C}\cdot\widetilde{C} = C\cdot C - \sum M(p_i) - \sum M(q_j) = 2\ell + 2$. Note that, by definition, at p_1 the last blow-up creates an exceptional divisor that intersects $\widetilde{C}$ at a single point with multiplicity ℓ.

Blow up ℓ more times at p_1, so that at p_1 we get to the normal crossing resolution of the singularity (C, p_1), and then $\ell + 1$ more times at the intersection between (the proper transform of) C and the last exceptional divisor. Let (X, ω) denote the corresponding blow-up of (X', ω').

The 4-manifold X contains the following configuration of symplectic spheres: a $+1$-sphere C', the proper transform of C, an exceptional divisor intersecting C transversely once, and a string of -2-curves departing from it; this is depicted in (6.1).

(6.1)

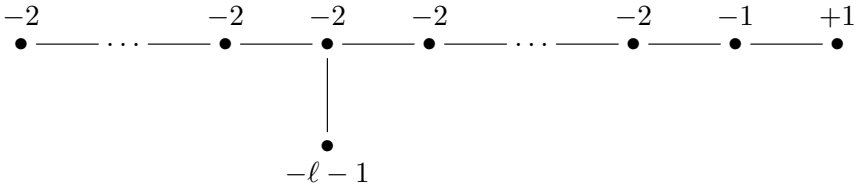

The left leg contains exactly $\ell - 1$ vertices of weight -2, while the right leg contains ℓ of them. In total, the chain of -2-vertices has length 2ℓ.

By Theorem 4.1, X is symplectomorphic to a blow-up of $\mathbb{CP}^2$, and C' can be identified with a line in $\mathbb{CP}^2$. Using the standard basis for $H_2(\mathbb{CP}^2 \# N\overline{\mathbb{CP}}^2)$, by Lemma 4.3 the -1-sphere adjacent to C' is in the homology class $h - e_0 - e_1$. Since the chain of -2s is of length $2\ell > 2$, by Lemma 4.6, up to relabeling the e_i, the homology classes in the chain are $e_1 - e_2, \ldots, e_{2\ell} - e_{2\ell+1}$. The central vertex in the plumbing is in the homology class $e_{\ell+1} - e_{\ell+2}$.

The $(-\ell - 1)$-sphere in (6.1) is disjoint from the line C', so by Lemma 4.3 its homology class is of the form $e_i - e_{j_1} - \cdots - e_{j_\ell}$ for some $i, j_1, \ldots, j_\ell$. It is also disjoint from the two halves of the chain of -2s, so the coefficients appearing in the homology class of the $(-\ell - 1)$-sphere of $e_1, \ldots, e_{\ell+1}$ are all equal—namely they are either all 0 or all -1. Since the $(-\ell - 1)$-sphere intersects the class $e_{\ell+1} - e_{\ell+2}$ once positively, either $i = \ell + 2$ or $j_k = \ell + 1$ for some k. The former possibility is ruled out by Lemma 4.5, therefore $e_1, \ldots, e_{\ell+1}$ must all appear with coefficient -1 in the homology class for the $(-\ell - 1)$-sphere. However, the self-intersection of this class is at most $-\ell - 2$, a contradiction. This proves the first assertion.

Note that when C is a rational cuspidal curve, i.e. if $\nu = 0$, the 3-manifold Y_C, that is the boundary of a regular neighborhood of C, is a rational homology sphere; in particular, since every weak symplectic filling of ξ_C can be deformed to a strong symplectic filling [OO99, Lemma 1.1], the last assertion follows. □

In fact we note here that for unicuspidal curves with a singularity of type $(\ell, \ell+1)$ the maximal self-intersection allowed by the proposition is $\ell^2 + 2\ell + 1 = (\ell+1)^2$, which is exactly the degree of the rational cuspidal curve $\{x^{\ell+1} - y^\ell z = 0\}$ of type $\mathcal{A}_\ell$. This shows that the inequality is sharp.

We give a small refinement of the proposition above for curves with more than one cusp.

Proposition 6.3. *Suppose that C is a rational curve with cusp singularities $p_1, \dots, p_\mu$ $(\mu > 1)$ such that $\ell(p_1) = \ell(p_2) = \min \ell(p_i)$, with reducible singularities $q_1, \dots, q_\nu$ $(\nu \geq 0)$, and self-intersection $C \cdot C$ satisfying*

$$C \cdot C \geq \sum M(p_i) + \sum M(q_j) + 2 \min \ell(p_i) + 1.$$

Then the associated contact structure ξ_C is not strongly symplectically fillable. If additionally $p_1, \dots, p_\mu$ are the only singularities of C, then ξ_C is not even weakly symplectically fillable.

Proof. Let $\ell = \ell(p_1) = \ell(p_2)$. Again, by Lemma 6.1, we can assume that $s(C) = \sum M(p_i) + \sum M(q_j) + 2 \min \ell(p_i) + 1$. As above, suppose that there is a filling (W, ω_W) of (Y_C, ξ_C) and glue it to a standard concave neighborhood of C to obtain the closed manifold (X', ω').

Blow up C at all its singular points until we obtain the minimal smooth resolution of C, i.e. the proper transform $\widetilde{C}$ of C is a smooth sphere of self-intersection $\widetilde{C} \cdot \widetilde{C} = C \cdot C - \sum M(p_i) - \sum M(q_j) = 2\ell + 2$. Note that, by definition, at p_1 and p_2 the last blow-up creates an exceptional divisor that intersects $\widetilde{C}$ at a single point with multiplicity ℓ.

Now blow up ℓ times at each of these latter tangency points to get to the normal crossing divisor resolution at p_1 and p_2, in the blown-up manifold (X, ω). By assumption, the proper transform of C is a symplectic $+1$-sphere, and by Theorem 4.1 we can identify it with a line in a blow-up of $\mathbb{CP}^2$. However, in X we see the following configuration.

(6.2)

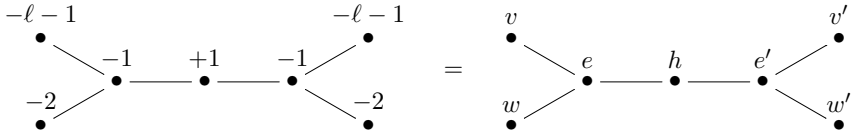

By Lemma 4.3 and 4.5, the vertices e, v, and w must be in the homology classes $h - e_1 - e_2$, $e_2 - e_3 - \cdots - e_{\ell+2}$, and $e_1 - e_0$, respectively. The class e' can either be in the homology class $h - e_1 - e_j$ or in the homology class $h - e_2 - e_j$, for some $j > 2$. In either case, we get a contradiction, because neither of the classes of v' or w' can be in a class $e_2 - \sum e_k$ or $e_1 - \sum e_k$, by Lemma 4.5.

This proves the first assertion. The second assertion follows verbatim as in the case of Proposition 6.2. □

The two propositions we have just proven give an upper bound for the self-intersection of a curve C with given singularities to exists in some closed symplectic 4-manifold. In particular, combining either of them with Lemma 6.1, we obtain that, if we fix the singularity types of a rational curve C, the set of integers s such that $s = C \cdot C$ for some C in a closed symplectic 4-manifold with those singularities is either empty or an interval $(-\infty, s_0]$.

In the rational and unicuspidal case, the existence of the Puiseux expansion shows that every singularity type is realized as one singularity of a rational plane curve, say C_0. Blowing up all the other singularities of C_0 (except for the desired one), one obtains a rational curve C_1 in a blow-up of $\mathbb{CP}^2$ that has one singularity of prescribed type. This shows in particular that, in the unicuspidal case, we always have an interval $(-\infty, s_0]$ of realized self-intersections, and Proposition 6.2 gives an upper bound on s_0.

Giving explicit lower bounds on s_0, however, is less easy. In the case of singularities of type (p, q), we can find the bound $s_0 > pq$. Indeed, the curve $\{x^p z^{q-p} - y^q = 0\}$ has degree q, and two singularities: one of type (p, q) at $(0 : 0 : 1)$, and the other of type $(q - p, q)$ at $(1 : 0 : 0)$. Taking the minimal smooth resolution of the latter, we obtain a curve C of self-intersection strictly larger than $q^2 - (q - p)q = pq$ (see [GS22, Lemma 2.4]), whose unique singularity is of type (p, q). Note that the self-intersection of the proper transform of C in the minimal smooth resolution of its only singularity, too, is positive (again, by [GS22, Lemma 2.4]).

Remark 6.4. A version of the two obstructions above was already known in the algebro-geometric context. Indeed, Hartshorne proved in [Har69, Theorem 4.1] that if an algebraic surface X contains a smooth genus-g curve C' of self-intersection at least $4g + 6$, then X is ruled, and C' is a section. The analogue result in the symplectic context has been proven by Kütle [Küt21]. For instance, this applies to the case of a rational curve C whose unique singularity is of type $(2, 3)$, and whose self-intersection is at least 10. To see this, observe that smoothing the singularity yields a genus-1 curve C' satisfying the requirements of Hartshorne's theorem, so C' is a section of a ruled

surface $X \to T^2$. Blow up once at the cusp of C and consider the map from the proper transform of C to T^2 obtained by composing the blow-down with the projection. This is a degree-1 map from a sphere to T^2, which gives a contradiction. This specific case was also known in the symplectic context, by work of Ohta and Ono [OO05].

In general, the bound obtained by applying Hartshorne's or Kütle's result is weaker than the one obtained by applying Proposition 6.2. This can be seen in the following family of examples: look at rational curves with only one singularity at p, which is of type (F_k, F_{k+1}). (As usual, F_k is the k^{th} Fibonacci number.) On the one hand, we have $4p_g(C) + 5 = 2(F_k - 1)(F_{k+1} - 1) + 5$, so Hartshorne's bound guarantees that there are no such curves as soon as the self-intersection s satisfies:

$$s \geq 2F_kF_{k+1} - 2F_k - 2F_{k+1} + 7.$$

On the other hand, the recursive definition of the Fibonacci numbers gives $\ell(p) = F_3 = 2$, so our bound implies that there can be no such rational curve when

$$s \geq M(p) + 2 \cdot 2 + 2 = \sum_{h=3}^{k} F_h^2 + 6 = F_kF_{k+1} + 4,$$

which is much smaller than the previous bound if k is large. (Here we have used the remarkable identity $\sum_{j=0}^{k} F_j^2 = F_kF_{k+1}$.)

7. Rational cuspidal curves of low arithmetic genus

In this section we look at symplectic filling classifications for contact manifolds (Y_C, ξ_C) where C is a rational cuspidal curve with low complexity, where we take arithmetic genus as our measure of complexity.

Recall from Section 4 that the arithmetic genus of a rational curve is determined by the multiplicity sequences of its singularities; each entry m in the sequence(s) contributes $\frac{1}{2}m(m-1)$ to the genus. If we restrict to low genus cases, this significantly restricts the types of singularities that may arise. We can vary the self-intersection number of the curve, s, freely (the curve will admit a concave neighborhood if $s > 0$), however we can only utilize techniques from [GS22] to classify fillings if s is sufficiently large to ensure that the proper transform of the curve in the minimal smooth resolution has positive self-intersection. Using the notation from Section 6, this means that we need $s > \sum_p M(p)$, where the sum is taken over all singular points p. Note that when the self-intersection gets sufficiently large

so that it exceeds the bounds of Proposition 6.2 or 6.3, the corresponding contact manifold is not fillable.

In this section, we consider all possible rational cuspidal curves C whose algebraic genus is at most three, with self intersection large enough so that the proper transform of the curve in the minimal resolution has strictly positive self-intersection. For each such curve, we classify the minimal symplectic fillings of the corresponding contact manifold (Y_C, ξ_C).

The reader is encouraged to review techniques and results from [GS22], as we will use them frequently in this section.

7.1. Genus 1

A rational cuspidal curve of arithmetic genus 1 can only have a single multiplicity sequence [2] singularity, which corresponds to type $(2, 3)$, i.e. a simple cusp. Suppose C is a rational cuspidal curve with a simple cusp as its unique singularity and self-intersection $s := C \cdot C$. For convenience, throughout this subsection we will denote the corresponding contact manifold by (Y_s, ξ_s) (though of course the contact manifold depends on the singularities specified).

The minimal smooth resolution results from a single blow-up at the cusp. The total transform consists of an exceptional divisor E of self-intersection -1 which is simply tangent to the smooth proper transform of C which has self-intersection $s - 4$. Therefore we constrain ourselves to the cases when $s \geq 5$.

Proposition 7.1. *Let (Y_s, ξ_s) be the contact boundary of a concave neighborhood of a rational cuspidal curve with a unique simple cusp, and self-intersection s.*

- *When $s = 5, 6, 7, 9$, (Y_s, ξ_s) has a unique minimal symplectic filling W and $b_2(W_s) = 9 - s$.*
- *When $s = 8$, (Y_s, ξ_s) has exactly two minimal symplectic fillings W_A and W_B, and $b_2(W_A) = b_2(W_B) = 1$.*
- *When $s \geq 10$, (Y_s, ξ_s) has no symplectic fillings.*

Proof. Since the multiplicity sequence for the unique singularity is [2], following the notation from Section 6, we have $M(p) = 4$ and $\ell(p) = 2$. Therefore, by Proposition 6.2, when $s \geq 10$, (Y_s, ξ_s) has no symplectic fillings.

For any minimal symplectic fillings W of (Y_s, ξ_s), we can glue W to a concave neighborhood of C to obtain a closed symplectic manifold X such

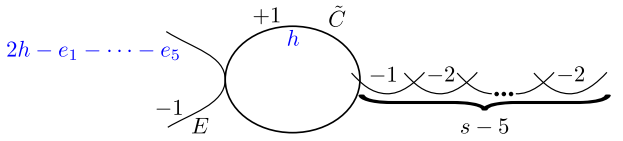

Figure 14. A blow-up of a curve C with a single simple cusp and self-intersection s, so that the proper transform $\widetilde{C}$ has self-intersection $+1$.

that the pair (X, C) is relatively minimal. Conversely, for any relatively minimal symplectic embedding of C into a closed symplectic manifold X, there is a concave neighborhood of C whose complement is a minimal symplectic filling of X. Therefore, to analyze the symplectic fillings when $5 \leq s \leq 9$, we classify relatively minimal symplectic embeddings of C into a closed symplectic manifold X. If C embeds in X, then we can blow up X, once at the singular point p to resolve the singularity of C, and $s-5$ times at another point q, so that the resulting proper transform $\widetilde{C}$ has self-intersection 1. See Figure 14.

By Theorem 4.1, there exists a symplectomorphism of $X\#(s-4)\overline{\mathbb{CP}}^2$ to $\mathbb{CP}^2\#N\overline{\mathbb{CP}}^2$ identifying the proper transform $\widetilde{C}$, a smooth symplectic sphere of self-intersection $+1$ with $\mathbb{CP}^1 \subset \mathbb{CP}^2$. Using the standard basis $\{h, e_1, \ldots, e_N\}$ for $H_2(\mathbb{CP}^2\#N\overline{\mathbb{CP}}^2)$, $[C] = h$. We determine the possible homology classes for the other components using the lemmas from section 4. By Lemma 4.3, the tangent exceptional sphere E represents $2h - e_1 - \cdots - e_5$. When $s > 5$, there is a chain of $s-5$ additional exceptional divisors. The first sphere in the chain is a -1-sphere intersecting C transversally and disjoint from E, and thus represents the class $h - e_1 - e_2$ (up to relabeling). By Lemma 4.6, the remaining spheres in the chain represent (a truncation of) $e_2 - e_3$, $e_3 - e_4$, $e_4 - e_5$ or in the case that $s = 8$ (so there are exactly two -2-spheres in the chain) they can represent $e_2 - e_3$, $e_1 - e_2$. In the first option, by Lemma 4.2, we can blow down *disjoint* exceptional spheres representing e_1 and $e_j, \ldots, e_5$ where j is the highest index appearing in the chain, such that these spheres have only positive intersections with the configuration. After these blow-downs, we can sequentially blow-down proper transforms of spheres *in the configuration* representing the remaining e_i classes. After blowing down all exceptional classes, the image of the total transform of C descends to a conic (the image of E) with one tangent line (the image of $\widetilde{C}$), and, when $s > 5$ another line intersecting the conic transversally in

two points (one is the image of $e_2, \dots, e_5$, and the other is the image of e_1) in $\mathbb{CP}^2$.

By [GS22, Proposition 5.1], such a configuration has a unique symplectic isotopy class in $\mathbb{CP}^2$. Therefore there is exactly one relatively minimal symplectic embedding (up to symplectic isotopy) of the total transform of C into $X\#(s-4)\overline{\mathbb{CP}}^2 \cong \mathbb{CP}^2\#5\overline{\mathbb{CP}}^2$ for each homological embedding. By deleting a concave regular neighborhood of the total transform of C, we get exactly one minimal symplectic filling of (Y_s, ξ_s) for each homological embedding. When $s = 5, 6, 7, 9$, this shows that there is a unique minimal symplectic filling, corresponding to the unique relatively minimal symplectic embedding of C into $\mathbb{CP}^2\#(5-(s-4))\overline{\mathbb{CP}}^2$. Since (Y_s, ξ_s) is a rational homology sphere, the Mayer–Vietoris long exact sequence implies the complementary filling has $b_2 = 9 - s$. By additivity of the signature, it is also negative definite.

When $s = 8$, there is the second homological embedding to consider, where the final -2-sphere in the chain represents $e_1 - e_2$. Using Lemma 4.2, we can find disjoint exceptional spheres in classes e_3, e_4, and e_5. After blowing these down, the proper transform of a sphere in the configuration represents e_2. Finally, after blowing down e_2, we find the proper transform of another sphere in the configuration represents e_1 and we blow this down. The resulting configuration is a conic (the image of E) and two distinct tangent lines (the images of $\widetilde{C}$ and of the first exceptional divisor in the chain, respectively). Again, by [GS22, Proposition 5.1], this configuration has a unique isotopy class in $\mathbb{CP}^2$, so we get a unique corresponding filling, that we call W_B. To see that the two corresponding fillings W_A (coming from the first embedding) and W_B are different, we look at their intersection forms. The torsion-free part of the former is generated by the class $e_1 - e_2 - e_3 - e_4 + 2e_5$, while that of the latter is generated by the class $e_4 - e_5$. In particular, the intersection forms of W_A and W_B are non-isomorphic, so W_A and W_B are non-diffeomorphic. □

Remark 7.2. Note that in the $s = 8$ case, the two homological embeddings of the total transform of C, correspond to two symplectic embeddings of C, one into $\mathbb{CP}^2\#\overline{\mathbb{CP}}^2$ and the other into $S^2 \times S^2$. The former embedding is obtained by blowing up a cuspidal cubic in $\mathbb{CP}^2$ at a non-singular point. The latter is obtained by taking a cuspidal cubic D and a line L meeting D transversely in three points, blowing up $\mathbb{CP}^2$ at two of them, and then contracting the proper transform of L. In our analyses, this will be a common source of multiple fillings of the same cuspidal contact manifold with the same Betti numbers.

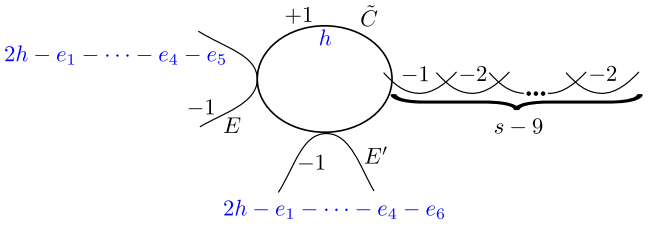

Figure 15. A blow-up of a curve C with a two simple cusps and self-intersection s, so that the proper transform $\widetilde{C}$ has self-intersection $+1$.

7.2. Genus 2

For a rational cuspidal curve of arithmetic genus 2, there can either be two simple cusps (each with multiplicity sequence $[2]$), or a single cusp which is a cone on a $(2,5)$-torus knot (multiplicity sequence $[2,2]$). In both cases, the minimal resolution results from two blow-ups at points of multiplicity 2, so we can classify symplectic fillings for such curves when the self-intersection number $s \geq 9$.

Proposition 7.3. *Let C be a rational cuspidal curve with self-intersection number s, such that either it has exactly two simple cusps or it has a unique singularity of type $(2,5)$, and let (Y_s, ξ_s) denote the corresponding cuspidal contact manifold.*

- *When $9 \leq s \leq 11$, (Y_s, ξ_s) has a unique minimal symplectic filling W_s, and $b_2(W_s) = 13 - s$.*
- *When $s = 12$, (Y_s, ξ_s) has exactly two minimal symplectic fillings, W_A and W_B, and $b_2(W_A) = b_2(W_B) = 1$.*
- *When $s \geq 13$, (Y_s, ξ_s) admits no symplectic fillings.*

Proof. We proceed with the same methods as used in the genus-1 case. The resolutions we embed into $X\#(s-7)\overline{\mathbb{CP}}^2 \cong \mathbb{CP}^2\#N\overline{\mathbb{CP}}^2$ are shown in Figures 15 and 16 for the two types of singularity configurations. In each case, we blow up a sufficient number of times so that the proper transform $\widetilde{C}$ has self-intersection 1, thus identifying $\widetilde{C}$ with $\mathbb{CP}^1 \subset \mathbb{CP}^2$ using Theorem 4.1.

In the case of two simple cusps, there are two tangent exceptional divisors of self-intersection -1 representing classes $2h - e_1 - \cdots - e_4 - e_5$ and

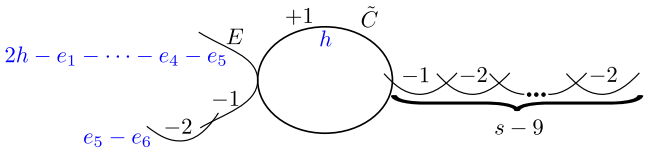

Figure 16. A blow-up of a curve C with a one cusp of type $(2, 5)$ and self-intersection s, so that the proper transform $\widetilde{C}$ has self-intersection $+1$.

$2h - e_1 - \cdots - e_4 - e_6$ by Lemma 4.3. By Lemmas 4.3 and 4.6, the exceptional divisors in the chain of length $s - 9$ represent classes $h - e_1 - e_2, e_2 - e_3, e_3 - e_4$ (Case 1), or $h - e_1 - e_2, e_2 - e_3, e_1 - e_2$ (Case 2) (when $s < 12$, the sequence is truncated and there is a unique option). In case 1, by Lemma 4.2, we can find disjoint exceptional spheres representing e_1, e_4, e_5, and e_6 (also e_3 or e_3 and e_2 if the sequence is truncated sufficiently such that these classes do not appear with positive coefficient in the configuration). Subsequently, we blow down spheres in the proper transform sequentially representing the remaining e_i.

Now we analyze the resulting configuration, which will consist of two conics (the images of E and E'), and two lines (the images of $\widetilde{C}$ and the curve representing $h - e_1 - e_2$. In the first homological embedding, when $s = 12$ the images of the exceptional spheres representing e_4, e_3, and e_2 will all be the same point (the image of the sphere representing e_4 will lie on the sphere representing e_3 and so on). When $s = 11$, the sphere representing e_4 is separated out but e_2 and e_3 have the same image, and when $s = 9, 10$, the spheres representing e_2, e_3, and e_4 are each sent to distinct points. In all cases, the spheres representing e_1, e_5, and e_6 can be realized disjointly from each other and all the other exceptional spheres and thus will be sent to distinct points. Since the two conics have positive intersection with e_2, e_3 and e_4, in the $s = 12$ case, their images under the blow-down will have a tangency of order 3 at the common image of e_2, e_3, and e_4. In the $s = 11$ case, the images of e_2 and e_3 will create a simple tangency and e_4 will correspond to a distinct transverse intersection. When $s = 9, 10$, e_2, e_3, and e_4 will correspond to three transverse intersections between the conics. In all cases, the conics will additionally intersect transversally at the image of e_1. The line given by the image of $\widetilde{C}$ will be tangent to each of the conics (as it was before blowing down). The other line will pass transversally through the two conics at two of their intersection points (the images of e_1 and e_2).

Omitting the last line, this configuration is $\mathcal{G}_3$, $\mathcal{G}_2$, or $\mathcal{G}_1$ from [GS22], which we proved has a unique symplectic isotopy class in [GS22, Propositions 5.5, 5.8, 5.9]. Adding in the last line, which is required to pass through two specific intersection points, we still have a unique symplectic isotopy class by [GS22, Proposition 5.1].

Next we consider case 2, (which is only distinct from the first when $s = 12$). In this case, we can blow down disjoint spheres representing e_3, e_4, e_5, and e_6 first, and then find sequential proper transforms representing e_2 then e_1 to blow down. Note that the images of the spheres representing e_1, e_2, and e_3 will land on the same point, and spheres representing e_4, e_5 and e_6 will be realized disjointly with distinct image points. The image point of e_1, e_2, and e_3 will be a tangency of order 3 between the two conics, and the curve which originally represented $h - e_1 - e_2$ will be tangent to these conics at this point. The image of e_4 will be a distinct transverse intersection between the conics. The image of $\widetilde{C}$ will be a line which is tangent to each of the two conics and transverse to the other line (all at points distinct from the previously specified intersections).

Thus the final configuration is again the $\mathcal{G}_3$ configuration with one additional line which is tangent to the conics at their triple tangency. Since, as mentioned above, the $\mathcal{G}_3$ has a unique symplectic isotopy class, the configuration with the additional tangent line also has a unique symplectic isotopy class by [GS22, Proposition 5.1].

When $9 \leq s \leq 11$, the unique relatively minimal symplectic embeddings correspond to unique minimal symplectic fillings of (Y_s, ξ_s) and the Betti number calculation follows from the Mayer–Vietoris long exact sequence and the fact that Y_s is a rational homology sphere. To distinguish the two fillings when $s = 12$, we can again look at the intersection form. For the homological embedding where the last sphere represents $e_3 - e_4$, the generator of the non-torsion part of the homology of the complement is $e_1 - e_2 - e_3 - e_4 + 2e_5 + 2e_6$ which has self-intersection -12. For the homological embedding where the last sphere represents $e_1 - e_2$, the generator of the non-torsion part of the homology of the complement is $e_4 - e_5 - e_6$ which has self-intersection -3.

We observe that it is not possible to find a homological embedding if there are more than two -2-spheres in the chain (i.e. when $s > 12$), since such a -2-sphere must represent a class $e_i - e_j$ which intersects $e_3 - e_4$ (or $e_1 - e_2$) once positively, and has intersection zero with all other curves in the configuration. Therefore, there are no symplectic embeddings of C into a closed symplectic manifold when $s \geq 13$, so (Y_s, ξ_s) has no symplectic fillings when $s \geq 13$. Note that Proposition 6.2 would only imply this for $s \geq 14$.

In the case of one cusp of type $(2,5)$, there is one exceptional divisor E of self-intersection -1 tangent to the proper transform $\widetilde{C}$, and another exceptional divisor E' of self-intersection -2 which intersects E once transversally and is disjoint from all other curves. Up to relabeling, $[E] = 2h - e_1 - \cdots - e_5$ and $[E'] = e_5 - e_6$. The exceptional divisors in the chain of length $s-9$ again represent classes $h - e_1 - e_2, e_2 - e_3, e_3 - e_4$ (case 1) or $h - e_1 - e_2, e_2 - e_3, e_1 - e_2$ (case 2).

In case 1, we can find disjoint exceptional spheres in classes e_1, e_4, and e_6 by Lemma 4.2 (and also e_3 or e_3 and e_2 if the sequence is sufficiently truncated). We blow these down and then sequentially blow down proper transforms of the spheres of the configuration representing the remaining exceptional classes. The resulting configuration is a single conic with one tangent line, and another line which intersects generically transversally. In case 2, we find disjoint exceptional spheres in classes e_3, e_4 and e_6 (with positive intersections with the configuration) and then after blowing these down, find sequentially proper transforms representing the other e_i and blow these down. The resulting configuration is a single conic with two distinct tangent lines. The resulting configurations in both cases have a unique symplectic isotopy class by [GS22, Theorem 1.5]. Thus this yields a unique symplectic filling when $9 \leq s \leq 11$. The two symplectic fillings corresponding to the two homological embeddings when $s = 12$ can be distinguished by their intersection forms, as their non-torsion homology is generated by $e_1 - e_2 - e_3 - e_4 + 2e_5 + 2e_6$ or $e_4 - e_5 - e_6$ respectively as in the previous case. Similarly, we obtain no possible homological embeddings when there are more than two -2-spheres in the chain so when $s \geq 13$, there are no symplectic fillings of (Y_s, ξ_s). □

7.3. Genus 3

When we allow the arithmetic genus of the rational cuspidal curve to increase to 3, there are more options for the types of cusps. The first option is to have a single cusp of type $(3,4)$ (multiplicity sequence $[3]$), where we consider self-intersection numbers $s \geq 10$. The second is to have a single cusp of type $(2,7)$ (multiplicity sequence $[2,2,2]$). The third option is to have two cusps, one a simple cusp (multiplicity sequence $[2]$) and the other of type $(2,5)$ (multiplicity sequence $[2,2]$). The fourth option is to have three simple cusps (each with multiplicity sequence $[2]$). In the second, third, and fourth options, we can classify fillings when the self-intersection number satisfies $s \geq 13$.

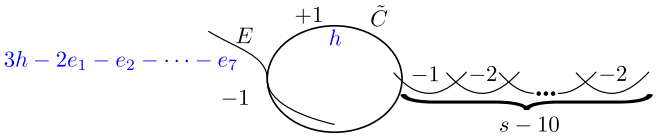

Figure 17. A blow-up of a curve C with a one cusp of type $(3, 4)$ and self-intersection s, so that the proper transform $\widetilde{C}$ has self-intersection $+1$.

Proposition 7.4. *Let C be a rational cuspidal curve with self-intersection s and a cusp of type $(3, 4)$ being the unique singularity, and let (Y_s, ξ_s) be the corresponding contact manifold.*

- *When $10 \leq s \leq 16$, (Y_s, ξ_s) has a unique minimal symplectic filling W and $b_2(W) = 16 - s$.*
- *When $s \geq 17$, (Y_s, ξ_s) is not symplectically fillable.*

Proof. That there are no fillings when $s \geq 17$ follows from Proposition 6.2.

For $10 \leq s \leq 16$, we proceed as in the lower genus cases. Blow up an embedding of C into X once at the cusp to get the minimal smooth resolution so that the exceptional sphere E is tangent with multiplicity 3 to the proper transform of C. We blow up $s - 10$ additional times at a different point so that $\widetilde{C}$ has self-intersection 1, yielding a chain of $s - 10$ exceptional spheres as in Figure 17. Identifying $\widetilde{C}$ with $\mathbb{CP}^1$ by Theorem 4.1 so $[\widetilde{C}] = h$, by Lemma 4.3, we see that $[E] = 3h - 2e_1 - e_2 - \cdots - e_7$, and the chain of $s - 8$ exceptional spheres represent the classes in (a truncation of) the sequence $h - e_1 - e_2, e_2 - e_3, e_3 - e_4, e_4 - e_5, e_5 - e_6, e_6 - e_7$. By Lemma 4.2, we can find disjoint exceptional spheres representing e_1 and $e_j, \ldots, e_7$ where j is the maximal index appearing in the chain, and then sequentially blow down proper transforms representing the remaining e_i. After this, E descends to a cubic curve with either a node or a cusp, $\widetilde{C}$ descends to an inflection line, and the first divisor in the chain descends to a line passing through the singular point of the cubic (the image of e_1) and one other point (the image of e_2). Without the last line, such a configuration has a unique symplectic isotopy class by [GS22, Proposition 5.11]. Note that a cusp can be locally deformed to a node through a symplectic family and after blowing up e_1, the proper transform in the cuspidal case is symplectically isotopic to that of the nodal case (and the proper transform is what corresponds to the resolution of C). We get a unique symplectic isotopy class for the configuration which

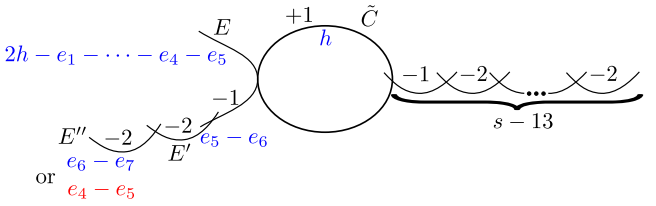

Figure 18. A blow-up of a curve C with a one cusp of type $(2,7)$ and self-intersection s, so that the proper transform $\widetilde{C}$ has self-intersection $+1$.

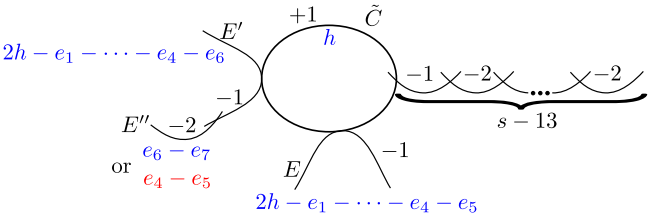

Figure 19. A blow-up of a curve C with a one cusp of type $(2,5)$ and one of type $(2,3)$ and self-intersection s, so that the proper transform $\widetilde{C}$ has self-intersection $+1$.

includes the last line by [GS22, Proposition 5.1]. Thus there is a unique relatively minimal symplectic embedding of this blow-up of C into a closed manifold and that manifold must be $\mathbb{CP}^2\#7\overline{\mathbb{CP}}^2$. We conclude that (Y_s,ξ_s) has a unique minimal symplectic filling with $b_2 = 16 - s$. □

Proposition 7.5. *Let C be a rational cuspidal curve with self-intersection s and either a unique $(2,7)$ cusp, or one $(2,3)$ cusp and one $(2,5)$ cusp, and let (Y_s,ξ_s) be the corresponding contact manifold.*

- *When $13 \le s \le 15$, (Y_s,ξ_s) has two minimal symplectic fillings W and W'. $b_2(W) = 16 - s$ and $b_2(W') = 17 - s$.*
- *When $s = 16$, (Y_s,ξ_s) has three minimal symplectic fillings W, W' and W''. $b_2(W) = 16 - s$ and $b_2(W') = b_2(W'') = 17 - s$.*
- *When $s \ge 17$, (Y_s,ξ_s) is not symplectically fillable.*

Proof. Proceeding as in prior cases, we blow up an embedding of C to its minimal resolution, then blow up $s-13$ additional times at another point until $\widetilde{C}$ has self-intersection 1 and can be identified with $\mathbb{CP}^1$. The three exceptional divisors from the minimal resolution must have homology classes as specified by the options shown in Figures 18 and 19 (depending on whether there are 1 or 2 cusps). Note that in both cases, there are two options for the homology class of the exceptional divisor E'': e_6-e_7 or e_4-e_5. Also for both cases, the homology classes of the divisors in the extra chain must represent either $h-e_1-e_2, e_2-e_3, e_3-e_4$ or $h-e_1-e_2, e_2-e_3, e_1-e_2$. If $[E'']=e_4-e_5$, the chain must take the second option. When $[E'']=e_6-e_7$, both options are possible, but note that they only differ when all three components are included corresponding to the $s=16$ case. Thus, we get three cases when $s=16$ and two cases when $13\leq s\leq 15$. We will call the case when $[E'']=e_4-e_5$ case 3, case 2 will have the chain ending in e_1-e_2, and case 1 will be the other option. Note, there are no allowed homological embeddings if the chain is longer, so (Y_s,ξ_s) has no fillings when $s\geq 17$.

First we look at the configuration coming from a curve with one $(2,7)$ cusp, where the resolution with its homological embedding is shown in Figure 18. For the homological embedding of case 1, we can first disjointly realize exceptional spheres in classes e_1, e_4, and e_7 (also e_3 or e_2 and e_3 if the chain is sufficiently truncated), and then sequentially blow down proper transforms representing the remaining e_i. The resulting configuration is a conic (the image of E) with one tangent line (the image of $\widetilde{C}$) and one generic secant line (the image of the first exceptional divisor in the chain). In case 2, we can blow down disjoint spheres representing e_3, e_4, and e_7, and then sequentially blow down proper transforms representing the remaining e_i. In case 3, we blow down disjoint spheres representing e_3 and e_6 and then sequentially blow down proper transforms representing the remaining e_i. In both cases 2 and 3, the resulting configuration is a conic with two distinct tangent lines. In both possible resulting configurations, there is a unique symplectic isotopy class by [GS22, Proposition 5.1]. Therefore each homological embedding corresponds to a unique symplectic isotopy class of embeddings.

Next, we consider the configuration coming from a curve with one $(2,3)$ cusp and one $(2,5)$ cusp. For the homological embedding of case 1, we blow down disjoint spheres in classes e_1, e_4, e_5, e_7 (and e_3 or e_2 and e_3 if sufficiently truncated), and then blow down proper transforms sequentially. In case 2, we blow down disjoint spheres in classes e_3, e_4, e_5, e_7, and then blow down proper transforms sequentially. In case 3, we blow down disjoint spheres in classes e_3, e_5, e_6 and then blow down proper transforms sequentially. The

configurations resulting from these blow-downs are exactly the same as those which arose in Propostion 7.3 in the case with two simple cusps, which all had unique isotopy classes (Case 1 here corresponds to Case 1 in 7.3, and Cases 2 and 3 here blow down to the same configuration as Case 2 from 7.3).

If $[E'']=e_6-e_7$, we have a relatively minimal symplectic embedding into $\mathbb{CP}^2\#7\overline{\mathbb{CP}}^2$. If $[E'']=e_4-e_5$ the relatively minimal embedding is into $\mathbb{CP}^2\#6\overline{\mathbb{CP}}^2$. Symplectic fillings complementary an embedding in $\mathbb{CP}^2\#7\overline{\mathbb{CP}}^2$ will have $b_2=17-s$, and those which are complementary to an embedding in $\mathbb{CP}^2\#6\overline{\mathbb{CP}}^2$ will have $b_2=16-s$. Thus, when $13\leq s\leq 15$, the two fillings have different b_2 so they are clearly not diffeomorphic. When $s=16$, there are two potential fillings with $b_2=17-s$. To distinguish these, we look at the square of the generator for the homology of the complement. In one case the generator is $e_1-e_2-e_3-e_4+2e_5+2e_6+2e_7$ of square -16 and in the other case the generator is $e_4-e_5-e_6-e_7$ of square -4. □

Remark 7.6. When $s=16$, in the minimal symplectic filling with $b_2=17-s=1$ where the homology class of E'' agrees with the option for the filling with $b_2=16-s=0$, we see that there is a symplectic -4-sphere in this filling representing the class $e_4-e_5-e_6-e_7$. Rationally blowing down this -4-sphere will yield another filling which is necessarily the unique rational homology ball filling. The other minimal symplectic filling with $b_2=17-s=1$ cannot be rationally blown-down (since there is no -4-sphere in a manifold with intersection form $\langle -16\rangle$).

Proposition 7.7. *Let C be a rational cuspidal curve with self-intersection s and three simple cusps, and let (Y_s,ξ_s) be the corresponding contact manifold.*

- *When $13\leq s\leq 16$, (Y_s,ξ_s) has a unique minimal symplectic filling W and $b_2(W)=16-s$.*
- *When $s\geq 17$, (Y_s,ξ_s) is not symplectically fillable.*

Proof. The determination of homological embeddings has a similar classification to the previous case. What is different in this situation is that not all of these homological embeddings correspond to actual geometric embeddings, and we need to prove a symplectic isotopy result for the ones which do. The possible homological embeddings are shown in Figure 20, where the additional chain of $s-13$ exceptional divisors represent classes $h-e_1-e_2$, e_2-e_3, and either e_3-e_4 or e_1-e_2. Note that when $[E'']=2h-e_1-e_2-e_3-e_5-e_6$, and $s=16$, the last divisor in the chain

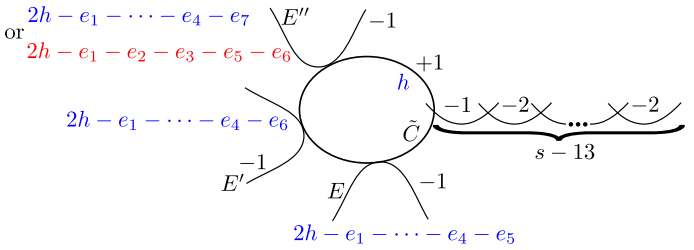

Figure 20. A blow-up of a curve C with a three cusps of type $(2, 3)$ and self-intersection s, so that the proper transform $\widetilde{C}$ has self-intersection $+1$.

must represent $e_1 - e_2$ to be disjoint from E''. Therefore we have three homological embeddings.

For the two homological embeddings where $[E''] = 2h - e_1 - \cdots - e_4 - e_7$, if we suppose this can be realized symplectically in $\mathbb{CP}^2 \# 7\overline{\mathbb{CP}}^2$, then we can blow down exceptional spheres so that the image in $\mathbb{CP}^2$ of the resolution becomes three symplectic conics in a pencil (the pencil points being the images of the exceptional spheres representing e_1, e_2, e_3, and e_4). When $s = 16$, one of the pencil points is a triple tangency of the conics and the other is a transverse intersection. When $s = 15$, one of the pencil points is a simple tangency and there are two other transverse pencil intersections. When $s = 13, 14$, there are four transverse pencil intersection points. Additionally, there is a symplectic line tangent to all three conics. When the pencil intersection points are all transverse, this is obstructed by [GS22, Proposition 5.22]. In the other two types of pencils, we can make a similar obstruction argument as follows.

In the case that there is a common simple tangency of the three conics in the pencil and two common transverse intersections, we obstruct this configuration as follows. Blow up once at each of the three pencil points where the conics intersect. The resulting proper transforms of the conics will intersect transversally at one common point, and will have self-intersection number $+1$. Thus we can identify one of them with a line in $\mathbb{CP}^2$. The other two necessarily represent the same homology class h (and thus are symplectic lines). The image of the line which was tangent to the three conics will represent $2h - e_1 - e_2 - e_3$. (There will also be three exceptional divisors representing homology classes $h - e_1 - e_2$, $h - e_1 - e_3$, and $h - e_2 - e_3$, but we will not actually need these for the obstruction.) Now, realize disjoint exceptional spheres representing e_1, e_2, and e_3, and blow them down. The

result is a configuration which includes a conic with three tangent lines that intersect at a common intersection point, which is the configuration $\mathcal{G}$ which is obstructed by [GS22, Proposition 5.21].

In the case that there is a triple tangency of the conics in the pencil, we obstruct this configuration similarly as follows. Blow up twice at the triple tangency of the conics and once at the transverse intersection. The proper transforms of the conics then have self-intersection $+1$ so we can identify them with lines in the homology class h, which intersect at a common point. Under this identification, what was originally a line will now be in homology class $2h - e_1 - e_2 - e_3$, and the exceptional spheres will represent $h - e_1 - e_2$, $h - e_1 - e_3$, and $e_1 - e_3$. Blowing down exceptional spheres representing e_1, e_2, and e_3 would yield a configuration with one conic and five lines. Three of these lines (the images of the original conics in the pencil) intersect the conic tangentially and intersect each other concurrently at a single point. Therefore this has a subconfiguration of type $\mathcal{G}$ which is obstructed by [GS22, Proposition 5.21]. Therefore these homological embeddings cannot be symplectically realized, so there are no corresponding symplectic fillings.

Now we consider the last remaining homological embedding where $[E''] = 2h - e_1 - e_2 - e_3 - e_5 - e_6$ and the chain represents a (truncation of) $h - e_1 - e_2$, $e_2 - e_3$, $e_1 - e_2$. We realize disjoint exceptional spheres in classes e_3, e_4, e_5, and e_6 and blow them down (if the chain is truncated we can also realize e_1 or e_1 and e_2 disjointly). The resulting configuration in $\mathbb{CP}^2$ consists of three symplectic conics C_1, C_2, C_3, and two symplectic lines L_1, and L_2. When $s = 16$, the images of the spheres representing e_1, e_2, and e_3 all coincide, so C_1, C_2, and C_3 intersect at one common triple tangency point p_3 (the image of e_1, e_2, and e_3) and a transverse double point for each of the three pairs (the images of e_4, e_5, e_6). In this case L_2 is tangent to the three conics at p_3. When $s = 15$, the images of e_2 and e_3 agree, so C_1, C_2, and C_3 intersect at one common simple tangency and one common (pencil) transverse intersection (along with the three double points for e_4, e_5, e_6). In this case L_2 intersects the conics transversally once at their common tangential intersection and once at their common transverse intersection. When $s = 13, 14$, the conics have three distinct common (pencil type) intersection points, and three pairwise double intersection points. In this case, L_2 passes through two of the common pencil intersection points. In all cases, L_1 is tangent to all three conics at other points.

First we consider the case when the conics have a common tangency of order 3. We will show this configuration is birationally equivalent to a conic

with four generic tangent lines. The conic with any number of generic tangent lines has a unique symplectic isotopy class by [GS22, Proposition 5.1]. Thus, demonstrating this birational equivalence suffices to prove this configuration has a unique symplectic isotopy class. To obtain the birational equivalence, blow up three times at the common triple tangency point p of the three conics. This creates three exceptional divisors in a chain with self-intersection numbers $-1, -2, -2$. The -1-curve intersects each of the proper transforms of the conics transversally once at distinct points, and the -2-curves are disjoint from the proper transforms of the conics. The line which was tangent to the conics at p will have proper transform of self-intersection number -1. It will intersect the -2-exceptional curve in the middle of the chain at one point transversally. It intersects the other line once transversally and is disjoint from the other curves. Thus we can blow down this -1-curve coming from the proper transform of L_2. The image of the -2-exceptional divisor from the middle of the chain after this blow-down becomes itself a -1-curve that we can blow down. After blowing it down, the other -2-exceptional divisor becomes a -1-curve that can be blown down. The resulting configuration is a conic (the image of L_1) with four tangent lines (three are the image of C_1, C_2, C_3 and the fourth is the image of the last exceptional divisor). See Figure 21.

Next we consider the case when the conics have a common tangency of order 2. To verify this configuration has a unique symplectic isotopy class in $\mathbb{CP}^2$, we add a symplectic line L_3 which is tangent to the three conics at their common tangential intersection—this does not change the symplectic isotopy classification by [GS22, Proposition 5.1]. We will show this configuration is birationally equivalent to a conic with four tangent lines and one additional line that passes transversally through the point where the fourth line is tangent to the conic (and otherwise has generic transverse double point intersections). This configuration has a unique symplectic isotopy class by [GS22, Proposition 5.1], so after we demonstrate the birational equivalence we will have verified the configuration we are interested in has a unique symplectic isotopy class. To see this birational equivalence, blow up once at the transverse pencil point of the conics and twice at the tangential pencil point. The images of L_2 and L_3 will be -1-spheres that we can blow down. After blowing these down, one additional exceptional divisor will represent a -1-sphere that can be blown down, and the resulting configuration is as claimed. See Figure 22.

Finally consider the case when the conics intersect transversally at three pencil points plus three double points. To verify this configuration has a unique symplectic isotopy class in $\mathbb{CP}^2$, we add two symplectic lines L_3,

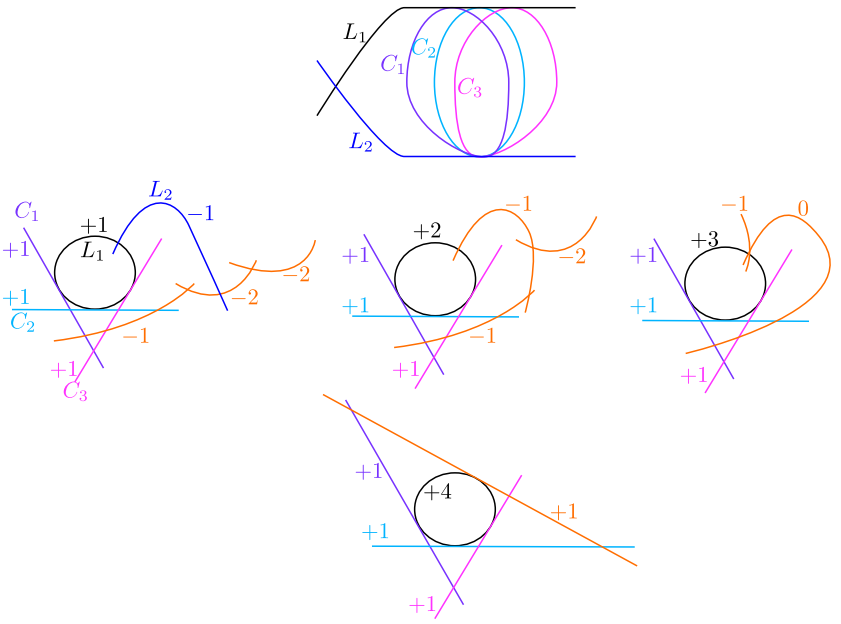

Figure 21. Birational equivalence from $\mathcal{A}$ (top) to $\mathcal{B}$ (bottom) where $\mathcal{A}$ consists of three conics intersecting at a common order 3 tangency at p, together with their tangent line at p, and another line which is tangent to all three conics and $\mathcal{B}$ consists of one conic with four generic tangent lines.

and L_4 pass through the other two pairs of pencil points (L_2 already passes through one of the three pairs). This does not change the symplectic isotopy classification by [GS22, Proposition 5.1]. We will show this configuration is birationally equivalent to a configuration with one conic, three tangent lines (forming a circumscribing triangle), and three more lines forming an inscribed triangle (i.e. the pairwise intersections of these three lines lie on the conic). Such a configuration can be built from the conic by iteratively adding a line satisfying the hypotheses of [GS22, Proposition 5.1], so it has a unique symplectic isotopy class. To see the birational equivalence, blow up at the three pencil points. The images of L_2, L_3, and L_4 become -1-spheres which can be blown down, resulting in the specified configuration. See Figure 23.

In conclusion, in each case, an embedding representing this homological configuration blows down to a configuration with a unique symplectic isotopy class. Thus there is a unique symplectic embedding of the cap with

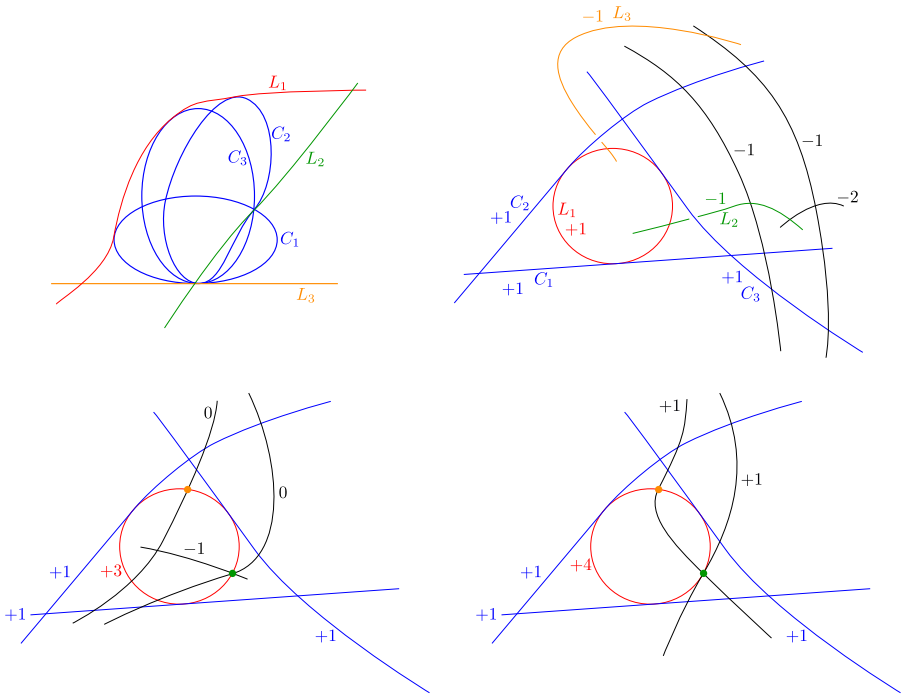

Figure 22. Birational equivalence starting with a configuration of three conics C_1, C_2, C_3 intersecting at one common simple tangency, one common transverse point, and three double points, together with three lines L_1, L_2, L_3 with tangencies and intersection data as shown in the top left. The ending configuration on the bottom right consists of one conic (the image of L_1) with five lines, four of which are tangent to the conic and the fifth passing transversally through one of the tangential intersections.

this homological data, corresponding to a unique symplectic filling in the complement. □

8. Further speculations and questions

We collect in this section some ideas and questions for further investigation.

8.1. Handlebodies

In Section 2 we gave explicit Stein handlebody descriptions for all rational homology ball fillings of the cuspidal contact structures associated to the

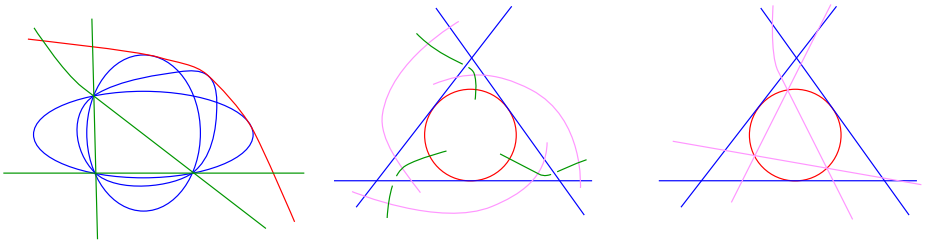

Figure 23. Birational equivalence between two configurations. The first configuration consists of three conics intersecting at three transverse pencil points and three double points, together with a line L_1 tangent to all three conics and three lines through the three pairs of pencil points. The final configuration consists of one conic, three tangent lines, and three lines whose pairwise intersections lie on the conic.

$\mathcal{A}_p$ and $\mathcal{B}_p$ families. Similar handlebody descriptions are known for rational homology balls bounded by lens spaces or by connected sums of lens spaces [LM14], thus covering also the two Fibonacci families of [FLMN07, Theorem 1.1] described in the introduction.

Question 8.1. Can one find an explicit Stein handlebody description of the rational homology ball fillings of $\mathcal{E}_3$ and $\mathcal{E}_6$?

In [AGLL20], there is a (somewhat non-explicit) handle decomposition of a topological rational homology ball bounding the corresponding Seifert fibered spaces. Starting from [AGLL20, Figure 7], one can recover a handlebody diagram for a rational homology ball bounding the cuspidal manifold of type $\mathcal{E}_3$, as shown in Figure 24. Does this handlebody support a Stein structure?

Note that it would suffice to Legendrian-realize the attaching curve of the 2-handle so that the contact framing is one less than the topological framing: that is, we are looking to find a Legendrian realization of the link of Figure 24 where the 2-handle has Thurston–Bennequin invariant -8 (in Gompf's convention [Gom98]). By the argument of Proposition 3.1, the contact structure obtained on the boundary would automatically be the canonical one (which is the cuspidal one, up to conjugation), and by the classification of fillings, such a diagram would represent the unique rational homology ball filling of (Y_C, ξ_C) where C is a curve of type $\mathcal{E}_3$.

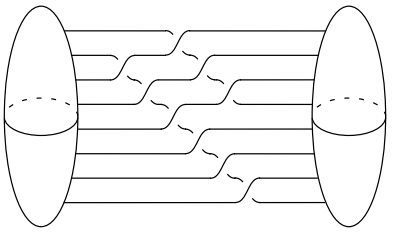

Figure 24. The handlebody description of a rational homology ball whose boundary is the cuspidal manifold of type $\mathcal{E}_3$. The framing of the 2-handle, in Gompf's convention from [Gom98], is -9.

8.2. Lefschetz fibrations and open books

In Sections 2 and 3 we have given explicit Stein handlebody decompositions for at least one filling for each curve of type $\mathcal{A}_p$, $\mathcal{B}_p$, $\mathcal{E}_3$, and $\mathcal{E}_6$. For the Fibonacci families, such descriptions were already known to Honda [Hon00] and Giroux [Gir00] (see also [LM14]).

Question 8.2. Can one construct explicit Lefschetz fibrations on these fillings?

As a byproduct, one would also be able to recover an open book decomposition for the cuspidal contact structures in this case. In fact, we conjecture that the diagrams in Figures 25 and 26 depict the vanishing cycles of the fillings in the $\mathcal{A}_p$ and $\mathcal{B}_p$ cases. We verified that the underlying topology is the expected one.

Moreover, adding the orange vanishing cycle in Figure 25 (respectively the orange vanishing cycle on the left of Figure 26) corresponds to attaching a Weinstein 2-handle along a Legendrian knot in $S^1 \times S^2$ which is in the same smooth isotopy class as the Legendrian knot in Figure 1 (respectively Figure 4). We see this by observing that Lefschetz fibrations without these orange curves destabilize to the trivial Lefschetz fibration on the annulus. In the $\mathcal{A}_p$ case, the Legendrian represented by the orange vanishing cycle is stabilized $p-1$ times, and the unstabilized version would correspond to the rational homology ball appearing in the standard rational blow-down corresponding to a daisy relation. Starting from a Stein handlebody diagram of this standard rational blow-down, it is not clear whether the Lefschetz fibration depicted represents positive or negative stabilizations of the Legendrian in that diagram, so there is some ambiguity remaining on whether

this is the correct Lefschetz fibration. Similar arguments can be made in the $\mathcal{B}_p$ case, and a similar ambuiguity remains.

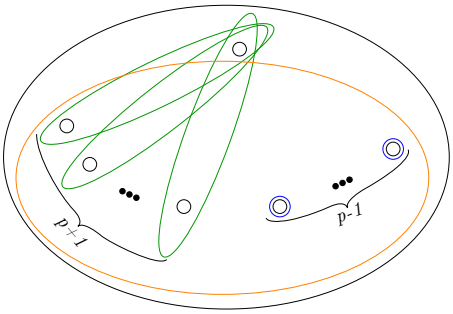

Figure 25. Lefschetz fibration for the filling corresponding to the $\mathcal{A}_p$ family.

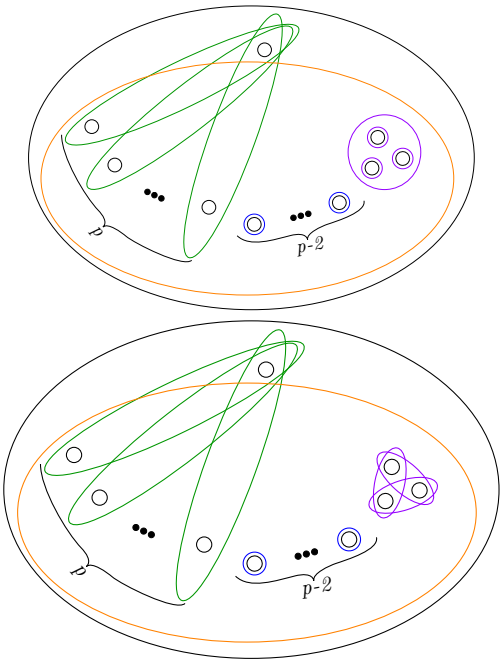

Figure 26. Lefschetz fibrations for the two fillings corresponding to the $\mathcal{B}_p$ family.

If the proposed open book decompositions do indeed describe the correct contact structures, we would also obtain that all cuspidal contact structures

of types $\mathcal{A}_p$, $\mathcal{B}_p$, or Fibonacci are supported by a planar open book. By contrast, by [GGP20, Theorem 1.2], we know that in the cases of $\mathcal{E}_3$ and $\mathcal{E}_6$ the cuspidal contact structures *cannot* be planar. On the other hand, Etnyre and Ozbagci have proved that these contact structures are supported by an open book of genus 1 [EO06].

References

[AGLL20] Paolo Aceto, Marco Golla, Kyle Larson, and Ana G. Lecuona. Surgeries on torus knots, rational balls, and cabling. To appear in *Ann. Inst. Fourier (Grenoble)*. Preprint `arXiv:2008.06760`, 2020.

[BCG16] József Bodnár, Daniele Celoria, and Marco Golla. Cuspidal curves and Heegaard Floer homology. *Proc. Lond. Math. Soc.*, 112(3):512–548, 2016.

[BO16] Mohan Bhupal and Burak Ozbagci. Symplectic fillings of lens spaces as Lefschetz fibrations. *J. Eur. Math. Soc. (JEMS)*, 18(7):1515–1535, 2016.

[BS11] Mohan Bhupal and András I. Stipsicz. Weighted homogeneous singularities and rational homology disk smoothings. *Amer. J. Math.*, 133(5):1259–1297, 2011.

[EG91] Yakov Eliashberg and Mikhael Gromov. Convex symplectic manifolds. In *Several complex variables and complex geometry, Part 2*, Proceedings of Symposia in Pure Mathematics, pages 135–162, 1991.

[Eli90] Yakov Eliashberg. Filling by holomorphic discs and its applications. In *Geometry of low-dimensional manifolds, 2 (Durham, 1989)*, volume 151 of *London Math. Soc. Lecture Note Ser.*, pages 45–67. Cambridge Univ. Press, Cambridge, 1990.

[EO06] John B. Etnyre and Burak Ozbagci. Open books and plumbings. *Int. Math. Res. Not. IMRN*, 2006:72710, 2006.

[FLMN07] Javier Fernández de Bobadilla, Ignacio Luengo, Alejandro Melle Hernández, and Andras Némethi. Classification of rational unicuspidal projective curves whose singularities have one Puiseux pair. In *Real and complex singularities*, Trends Math., pages 31–45. Birkhäuser, Basel, 2007.

[FS97] Ronald Fintushel and Ronald J. Stern. Rational blowdowns of smooth 4-manifolds. *J. Differential Geom.*, 46(2):181–235, 1997.

[FS06] Ronald Fintushel and Ronald J. Stern. Double node neighborhoods and families of simply connected 4-manifolds with $b^+ = 1$. *J. Amer. Math. Soc.*, 19(1):171–180, 2006.

[GGP20] Paolo Ghiggini, Marco Golla, and Olga Plamenevskaya. Surface singularities and planar contact structures. *Ann. Inst. Fourier (Grenoble)*, 70(4):1791–1823, 2020.

[Ghi08] Paolo Ghiggini. On tight contact structures with negative maximal twisting number on small Seifert manifolds. *Algebr. Geom. Topol.*, 8(1):381–396, 2008.

[Gir00] Emmanuel Giroux. Structures de contact en dimension trois et bifurcations des feuilletages de surfaces. *Invent. Math.*, 141(3):615–689, 2000.

[GK22] Marco Golla and Fabien Kütle. Symplectic isotopy of rational cuspidal sextics and septics. *Int. Math. Res. Not. IMRN*, 2022. Preprint, `arXiv:2008.10923`.

[Gom98] Robert E. Gompf. Handlebody construction of Stein surfaces. *Ann. of Math. (2)*, 148(2):619–693, 1998.

[GS99] Robert E. Gompf and András I. Stipsicz. *4-manifolds and Kirby calculus*, volume 20 of *Graduate Studies in Mathematics*. American Mathematical Society, Providence, RI, 1999.

[GS22] Marco Golla and Laura Starkston. The symplectic isotopy problem of for rational cuspidal curves. *Compos. Math.*, 158(7):1595–1682, 2022.

[Har69] Robin Hartshorne. Curves with high self-intersection on algebraic surfaces. *Publ. Math. I.H.E.S.*, 36:111–125, 1969.

[Hon00] Ko Honda. On the classification of tight contact structures, I. *Geom. Topol.*, 4(1):309–368, 2000.

[Kap79] Steve J. Kaplan. Constructing framed 4-manifolds with given almost framed boundaries. *Trans. Amer. Math. Soc.*, 254:237–263, 1979.

[Küt21] Fabien Kütle. *Courbes symplectiques de haute auto-intersection dans les surfaces symplectiques*. PhD thesis, Université de Nantes, 2021. Preprint, `arXiv:2111.04836`.

[Lis08] Paolo Lisca. On symplectic fillings of lens spaces. *Trans. Amer. Math. Soc.*, 360(2):765–799, 2008.

[Liu14] Tiankai Liu. *On planar rational cuspidal curves*. PhD thesis, Massachussets Institute of Technology, 2014.

[LM14] Yankı Lekili and Maksim Maydanskiy. The symplectic topology of some rational homology balls. *Comment. Math. Helv.*, 89(3):571–596, 2014.

[LS04] Paolo Lisca and András I. Stipsicz. Ozsváth-Szabó invariants and tight contact three-manifolds. I. *Geom. Topol.*, 8:925–945, 2004.

[Mat18] Irena Matkovič. Classification of tight contact structures on small Seifert fibered L-spaces. *Algebr. Geom. Topol.*, 18(1):111–152, 2018.

[McD90] Dusa McDuff. The structure of rational and ruled symplectic 4-manifolds. *J. Amer. Math. Soc.*, 3(3):679–712, 1990.

[Mos71] Louise Moser. Elementary surgery along a torus knot. *Pacific J. Math.*, 38(3):737–745, 1971.

[OO99] Hiroshi Ohta and Kaoru Ono. Simple singularities and topology of symplectically filling 4-manifold. *Comment. Math. Helv.*, 74:575–590, 1999.

[OO05] Hiroshi Ohta and Kaoru Ono. Symplectic 4-manifolds containing singular rational curves with $(2, 3)$-cusp. *Sémin. Congr.*, 10:233–241, 2005.

[OS12] Brendan Owens and Sašo Strle. Dehn surgeries and negative-definite four-manifolds. *Selecta Math. (N.S.)*, 18(4):839–854, 2012.

[OSz03] Peter S. Ozsváth and Zoltán Szabó. Absolutely graded Floer homologies and intersection forms for four-manifolds with boundary. *Adv. Math.*, 173(2):179–261, 2003.

[OSz04] Peter Steven Ozsváth and Zoltán Szabó. Holomorphic disks and topological invariants for closed three-manifolds. *Ann. of Math. (2)*, 159(3):1027–1158, 2004.

[OSz05] Peter S. Ozsváth and Zoltán Szabó. Heegaard Floer homology and contact structures. *Duke Math. J.*, 129(1):39–61, 2005.

[Par97] Jongil Park. Seiberg-Witten invariants of generalised rational blow-downs. *Bull. Austral. Math. Soc.*, 56(3):363–384, 1997.

[Par05] Jongil Park. Simply connected symplectic 4-manifolds with $b_2^+ = 1$ and $c_1^2 = 2$. *Invent. Math.*, 159(3):657–667, 2005.

[PSS05] Jongil Park, András I. Stipsicz, and Zoltán Szabó. Exotic smooth structures on $\mathbb{CP}^2\#5\overline{\mathbb{CP}^2}$. *Math. Res. Lett.*, 12(5-6):701–712, 2005.

[SS05] András I. Stipsicz and Zoltán Szabó. An exotic smooth structure on $\mathbb{CP}^2\#6\overline{\mathbb{CP}^2}$. *Geom. Topol.*, 9:813–832, 2005.

[SSW08] András I. Stipsicz, Zoltán Szabó, and Jonathan Wahl. Rational blowdowns and smoothings of surface singularities. *J. Topol.*, 1(2):477–517, 2008.

[Sym98] Margaret Symington. Symplectic rational blowdowns. *J. Differential Geom.*, 50(3):505–518, 1998.

[Sym01] Margaret Symington. Generalized symplectic rational blowdowns. *Algebr. Geom. Topol.*, 1:503–518, 2001.

[Tos20] Bülent Tosun. Tight small Seifert fibered spaces with $e_0 = -2$. *Algebr. Geom. Topol.*, 20(1):1–27, 2020.

[Tur02] Vladimir Turaev. *Torsions of* 3*-dimensional manifolds*, volume 208 of *Progress in Mathematics*. Birkhäuser Verlag, Basel, 2002.

[Wal04] C. T. C. Wall. *Singular points of plane curves*, volume 63. Cambridge University Press, 2004.

[Wen10] Chris Wendl. Strongly fillable contact manifolds and J-holomorphic foliations. *Duke Math. J.*, 151(3):337–384, 2010.

Laboratoire de mathématiques Jean Leray
CNRS and Nantes Université
44322 Nantes, France
E-mail address: marco.golla@univ-nantes.fr

Department of Mathematics, UC Davis
Davis, CA 95616, USA
E-mail address: lstarkston@math.ucdavis.edu

Received December 12, 2021
Accepted March 2, 2024